Russian Chemical Reviews **71** (6) 439 – 463 (2002) © 2002 Russian Academy of Sciences and Turpion Ltd

DOI 10.1070/RC2002v071n06ABEH000721

Phase equilibria, phases and chemical compounds in the Ti – C system

A I Gusev

Contents

I. Introduction 439
II. Phase diagrams of the Ti – C system at temperatures above 1000 K and thermodynamic properties of disordered titanium monocarbide TiC_y 440
III. New chemical compounds in the Ti – C system 448
IV. Ordered phases of nonstoichiometric titanium carbide TiC_y 452
V. Phase diagrams of the Ti – C system constructed with allowance for the ordering of TiC_y 458
VI. Conclusion 460

Abstract. The results of experimental and theoretical investigations of the phase equilibria in the titanium – carbon system are generalised. The generalised thermodynamic characteristics of disordered titanium carbide, TiC_y, are reported. Peculiarities of the crystal structures of all the known and hypothetical compounds of titanium with carbon are considered in detail. The X-ray diffraction patterns which allow identification of all these compounds are presented. The phase diagrams of the Ti – C system constructed with allowance for atomic ordering of nonstoichiometric carbide, TiC_y, and for the existence of the molecular cluster-like compounds Ti_8C_{12} and $Ti_{13}C_{22}$ (TiC_2) are discussed. The bibliography includes 142 references.

I. Introduction

Carbides of Group IV and V transition *d*-metals belong to strongly nonstoichiometric interstitial compounds.[1–3] A typical representative of strongly nonstoichiometric compounds is cubic titanium monocarbide TiC_y ($0.48 \leqslant y \leqslant 1.00$) with the *B*1-type structure, which has found wide practical applications and has been the subject of intensive experimental and theoretical research.

In 1823, Wollaston reported the discovery of pure crystalline titanium in metallurgic slags. However, after a lapse of 33 years Wöhler (Germany) showed that these crystals were titanium carbide containing nitrogen impurity. More recently in the 19th century contaminated titanium carbide was extracted from titanium-containing cast iron.[4,5] Some attempts at obtaining pure titanium carbide by carbothermal reduction of titanium dioxide, TiO_2, were also made (see Ref. 6).

The history of studies of titanium carbide and the Ti – C system can arbitrarily be divided into three periods.

In the first period (from the middle 1850s up to 1940), titanium carbide as well as the carbides and nitrides of other transition metals (zirconium, hafnium, vanadium, niobium, tantalum) were treated as ordinary chemical compounds of stoichiometric composition. Most studies carried out in this period were related to the establishment of the types of crystal structure and to the determination of the unit cell parameters of the titanium carbide samples obtained in one way or another. Titanium carbide was assumed to have a stoichiometric composition TiC. By the end of the first period, investigations of the thermodynamic and various physical properties of carbides and nitrides began and massive discrepancies between the results of different studies of the properties of titanium carbide were revealed. These discrepancies could not be rationalised by the measurement errors or by differences in the experimental methods. Detailed crystal-chemical studies showed that the discrepancies were due to the different content of carbon atoms in the carbide. It was found that, in contrast to other compounds, the composition of titanium carbide and, broadly, of the Group IV and V transition metal carbides and nitrides can vary over a very wide range while their crystal structure remains unchanged. In particular, the composition of titanium monocarbide TiC_y can vary from $TiC_{0.48}$ to $TiC_{1.00}$.

In the second period (from 1940 to 1970s), emphasis was mainly placed on investigations of the composition – property correlations for strongly nonstoichiometric compounds (in particular, interstitial phases). Interest in the carbides peaked in the 1960s, when thousands of communications were reported, concerning the effect of composition on the crystal-chemical, thermodynamic, thermal-physical, electrical, magnetic, optical, mechanical and other properties of these substances. By this time, the main qualitative concepts of the nature of chemical bonding in nonstoichiometric carbides have been developed. In the 1970s, the number of publications concerning basic problems relating to nonstoichiometric carbides reduced considerably; however, this time was characterised by increasing interest in applied studies. Titanium carbide had found wide use in production of hard alloys for metal-cutting tools. Most of the researchers erroneously concluded that there was almost nothing left to study in nonstoichiometric carbides. The first (tentative) variants of the phase diagram of the Ti – C system were reported,[7,8] which reflected the existence of the only compound, *viz*., cubic titanium monocarbide, TiC_y, with a broad homogeneity region. These phase diagrams remained nearly unchanged up to the mid-1990s.

For a long time after nonstoichiometric compounds were shown to have broad homogeneity regions, it was assumed that non-metal interstitial atoms and structural vacancies (unoccupied interstices of the metal sublattice) were randomly distributed over the lattice. However, crystallographic studies reported in 1967 (see Ref. 9) and more recently revealed that under particular condi-

A I Gusev Institute of Solid State Chemistry, Urals Branch of the Russian Academy of Sciences, ul. Pervomaiskaya 91, 620219 Ekaterinburg, Russian Federation. Fax (7-343) 274 44 95. Tel. (7-343) 274 73 06, (7-343) 249 35 23. E-mail:gusev@ihim.uran.ru

Received 4 April 2002
Uspekhi Khimii **71** (6) 507 – 532 (2002); translated by A M Raevsky

tions the interstitial atoms and vacancies can be redistributed over the sites of the crystal lattice, thus forming different types of ordered structures. The ordering of carbon atoms and structural vacancies was first observed in nonstoichiometric titanium carbide.[9]

In the late 1960s, the third period began of studies of nonstoichiometric compounds, which is mainly related to investigations into the ordering and its influence on the properties of these systems. Currently, one can say with certainty that at temperatures below 1000 K nonstoichiometric carbides and nitrides exist in the thermodynamically equilibrium ordered state, whereas their disordered state is metastable in the same temperature range.

In the 1980s, research into correlations between the properties of strongly nonstoichiometric compounds and the character of distribution of the interstitial atoms and vacancies began. It was shown that the effect of atomic and vacancy ordering on changes in the properties of a nonstoichiometric compound is comparable with the effect of varying the composition of the same system within the homogeneity region of the ordered phase. Therefore, varying the composition and redistribution of the atoms and vacancies in the crystal lattice of strongly nonstoichiometric compounds are two ways of controlling the properties of these compounds that possess equal rights.

A large number of ordered phases of strongly nonstoichiometric compounds was found during the decade from 1990 to 2000. The results of experimental studies and calculations of the phase equilibria allowed construction of the phase diagrams of the M–C and M–N (M = Ti, Zr, Hf, V, Nb, Ta) systems with allowance for both the presence of strongly nonstoichiometric carbides (MC_y) and nitrides (MN_y) and their ordering at temperatures below 1300 K (see Refs 1–3 and 10–27).

In 1992, a novel class of molecular metal–carbon nanoclusters was discovered.[28–38] Three stable molecular clusters — Ti_8C_{12}, $Ti_{13}C_{14}$ and $Ti_{13}C_{22}$ — were obtained in the Ti–C system. Some experimental and theoretical studies on titanium dicarbide, TiC_2, were also reported.

Thus, the last two decades are characterised by avalanche-like growth of the body of information on the phase equilibria and compounds in the Ti–C system. The phase diagram of this system was found to be much more intriguing and complicated than it was assumed previously. The aim of this review was to generalise the results of recent (reported between 1980 and 2000) experimental and theoretical investigations of chemical compounds and phases in the Ti–C system taking into account all available information. The emphasis is placed on the phase equilibria in this binary system and on the crystal structure of both the known and theoretically possible (model) phases and compounds of carbon and titanium.

II. Phase diagrams of the Ti–C system at temperatures above 1000 K and thermodynamic properties of disordered titanium monocarbide TiC_y

1. Phase diagrams

No phase diagrams of the Ti–C system constructed with allowance for the ordering of nonstoichiometric carbide TiC_y were reported until the mid-1990s. In the text below we will consider the principal results of investigations into the phase equilibria in the Ti–C system at temperatures above the ordering temperature of nonstoichiometric titanium carbide (*i.e.*, at $T > 1000$ K).

Detailed studies of phase equilibria in binary carbide-forming M–C (M is a transition metal) systems were mostly carried out in 1961–1965.[39] Up to now, the experimental results [including those for the Ti–C system at temperatures above 1800 K (see Ref. 7)] obtained at that time are the most reliable and accurate.

The phase diagram of the Ti–C system is presented in Fig. 1. In this system, cubic titanium carbide TiC_y with the *B*1-type

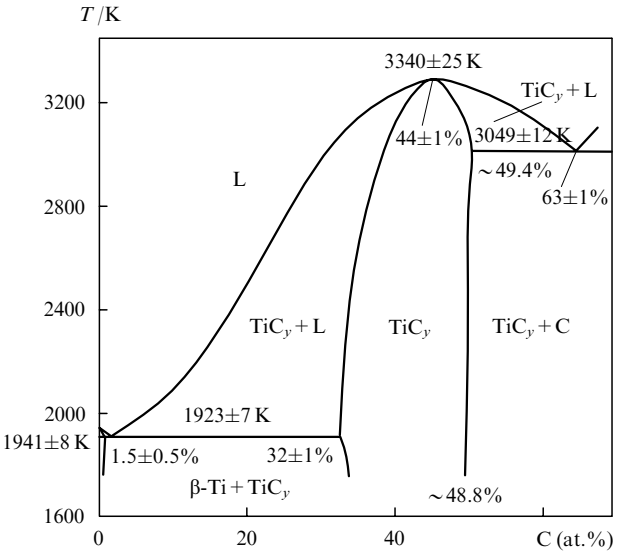


Figure 1. Experimental phase diagram of the Ti–C system at $T > 1800$ K.[7]

structure is in equilibrium with β-Ti (bcc structure) or α-Ti (hcp structure).

The melting temperature of pure metallic β-Ti is 1941±8 K (see Ref. 7). The addition of carbon to titanium reduces the melting temperature of Ti down to the eutectic temperature [1918 ± 5,[40] 1923 ± 7,[7] 1921 ± 5,[41–43] 1925 K (see Ref. 44)]. The eutectic $L \leftrightarrows$ β-Ti + TiC_y was reported to contain 4.4 at.% of carbon;[40] however, metallographic tests[7] showed that the content of carbon in the eutectic is 1.5 ± 0.5 at.%. Difficulties in determination of the eutectic composition by metallographic tests have been pointed out.[7, 39]

Allotropic transformation α-Ti $\leftrightarrows$ β-Ti occurs at 1155 ± 5 K (see Ref. 8). The addition of carbon to titanium causes an increase in the temperature of this transformation up to the temperature of the β-Ti + $TiC_y \leftrightarrows$ α-Ti peritectoid transformation, which equals 1193 ± 3 K (see Refs 41–43) or 1205 K (see Ref. 44).

At temperatures above 1000 K, there is only one nonstoichiometric compound in the binary system Ti–C, *viz.*, cubic titanium carbide TiC_y with a very broad homogeneity region from $TiC_{0.47}$ to $TiC_{0.96}$ at $T \approx 1920$ K.[7, 39] Raising the temperature up to 3000 K causes a shift of both the lower and upper bounds of the homogeneity region of TiC_y towards a higher content of carbon. At $T \approx 3000$ K, the upper bound of the homogeneity region corresponds to a $TiC_{0.998}$ composition (see Ref. 8). The highest melting temperature, 3340 ± 15 K (see Refs 7, 39, 41–43) or 3341 K (see Ref. 44), has carbide $TiC_{0.80}$ which undergoes congruent melting. The temperature of the $L \leftrightarrows TiC_y$ + C eutectic containing ~63 at.% of carbon is 3049 ± 12 K,[7] 3049 ± 6 K (see Refs 39, 41, 42) or 3048 K (see Ref. 44).

Figure 2 presents the phase diagram of the Ti–C system constructed by Murray[41, 42] for $T > 800$ K. The same phase diagram was also reported in a reference guide.[43] Most of the phase equilibria in this diagram were shown tentatively. Murray supplemented the phase diagram shown in Fig. 1 with some essential details by indicating the regions of allotropic transformation α-Ti $\leftrightarrows$ β-Ti and peritectoid transformation β-Ti + $TiC_y \leftrightarrows$ α-Ti. On the other hand, the phase diagram of this system (see Fig. 2) contained a tentatively shown existence region of ordered Ti_2C phase that was thought to exist and be stable at temperatures below 2170 K.[9, 45] However, the first report[9] on the stability of the ordered Ti_2C phase at $T \leqslant 2170$ K was found to be erroneous: more recently, numerous studies of the ordering of nonstoichiometric carbide TiC_y revealed that cubic ordered Ti_2C phase (space group C_{4h}^5) is formed at temperatures below 1000 K (see, *e.g.*, Refs 12, 21, 46–56). At $T < 1000$ K,

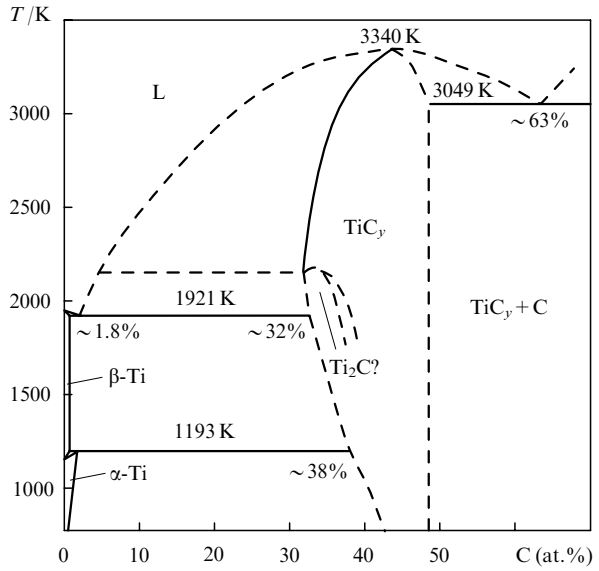


Figure 2. Phase equilibria in the Ti–C system at $T > 800$ K.[41–43] Ti_2C is the ordered phase of nonstoichiometric titanium carbide TiC_y.

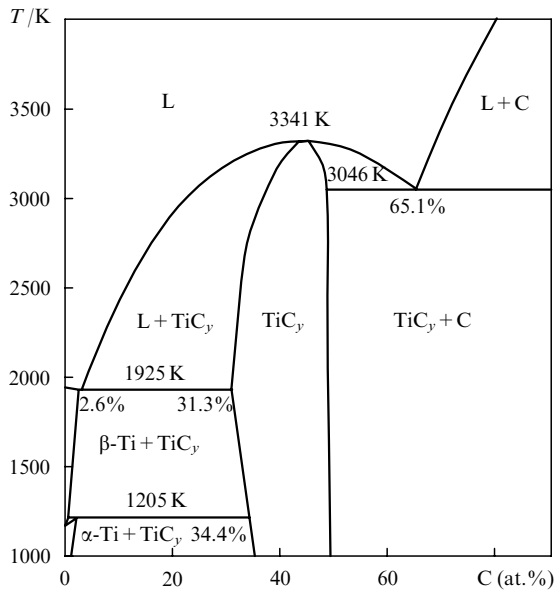


Figure 3. Phase diagram of the Ti–C system at $T > 1000$ K calculated [44] taking into account the results of experimental studies.[7, 8, 39]

there are several ordered phases in the homogeneity region of carbide TiC_y that are not shown in this phase diagram.

Phase equilibria in the system under study at temperatures above 1000 K have most reliably been shown in the phase diagram calculated by Jonsson [44] taking into account the experimental data reported by Rudy *et al.*[7, 39] Jonsson's phase diagram is shown in Fig. 3. The results of investigations of the crystal structure of different phases and the characteristics of special points of the phase diagram of the Ti–C system at $T > 1000$ K are listed in Tables 1 and 2, respectively.

Table 1. Crystal structure of phases that exist in the Ti–C system at $T > 1000$ K.

Phase	Existence region [C (at.%)]	Space group	Pearson notation	Lattice type
β-Ti	0–0.6	$Im\bar{3}m$ (O_h^9)	*cI*2	*A*2 (W)
α-Ti	0–1.6	$P6_3/mmc$ (D_{6h}^4)	*hP*2	*A*3 (Mg)
TiC_y	~32.0–49.8	$Fm\bar{3}m$ (O_h^5)	*cF*8	*B*1 (NaCl)
C	100	$P6_3/mmc$ (D_{6h}^4)	*hP*4	*A*9 (graphite)

Table 2. Characteristics of special points in the phase diagram of the Ti–C system at $T > 1000$ K.

Phase transformation	Composition of phases involved in reaction [C (at.%)]			T /K	Phase transformation type
L ⇆ β-Ti + TiC_y	1.8	0.6	32	1918 ± 5	eutectic transformation
L ⇆ TiC_y	–	44.4	–	3340 ± 15	congruent melting
L ⇆ TiC_y + C	65.1	48.5	~100	3050 ± 6	eutectic transformation
β-Ti + TiC_y ⇆ α-Ti	0.4	34.4	2.1	1193 ± 3	peritectoid transformation
L ⇆ β-Ti	–	0	–	1941 ± 8	melting
β-Ti ⇆ α-Ti	–	0	–	1155 ± 5	allotropic transformation

2. Structure and thermodynamic properties of disordered titanium carbide

a. Structure

Disordered cubic titanium monocarbide TiC_y with the *B*1-type structure is the most important chemical compound that exists in the Ti–C system at temperatures above 1000 K. The unit cell of TiC_y comprises two face-centred (metal and non-metal) sublattices displaced by half the lattice constant with respect to each other (Fig. 4). All sites in the metal sublattice of TiC_y are occupied by titanium atoms. The number of sites in the non-metal (carbon) sublattice is larger than that of interstitial atoms (*i.e.*, carbon atoms), which is typical of nonstoichiometric compounds. In the disordered state, which is in thermodynamic equilibrium only at $T > 1000$ K and is treated as a quenched metastable state at lower temperatures, carbon atoms are randomly distributed over the sites. The non-metal sublattice is characterised by the same site occupation probability equal to the value of y (the relative content of carbon in the carbide). This is responsible for the retention of cubic symmetry of the disordered non-metal sublattice and means that all sites in the carbon sublattice of disordered TiC_y are crystallographically equivalent. A typical X-ray diffraction pattern of homogeneous cubic titanium carbide is shown in Fig. 5. The lattice constant of TiC_y nonmonotonically increases as the content of carbon increases (Fig. 6).[57]

Nonstoichiometric titanium carbide can possess quite different thermodynamic properties within the homogeneity region. Therefore, of particular value are those studies in which the

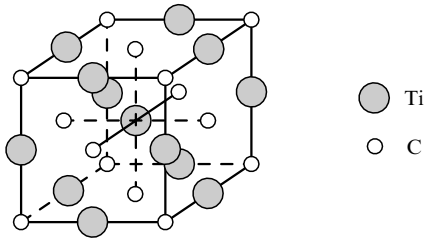


Figure 4. Unit cell of cubic disordered nonstoichiometric TiC_y with the *B*1(NaCl)-type structure. All sites in the metal sublattice are occupied by Ti atoms, while the sites in the non-metal sublattice are randomly occupied by C atoms.

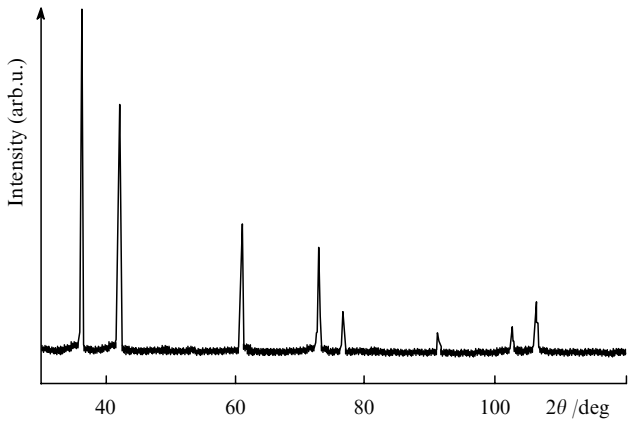


Figure 5. X-Ray diffraction pattern of disordered titanium carbide $TiC_{0.52}$ with cubic $B1$-type structure (a_{B1} = 0.4306 nm, Cu$K_{\alpha 1,2}$ radiation).

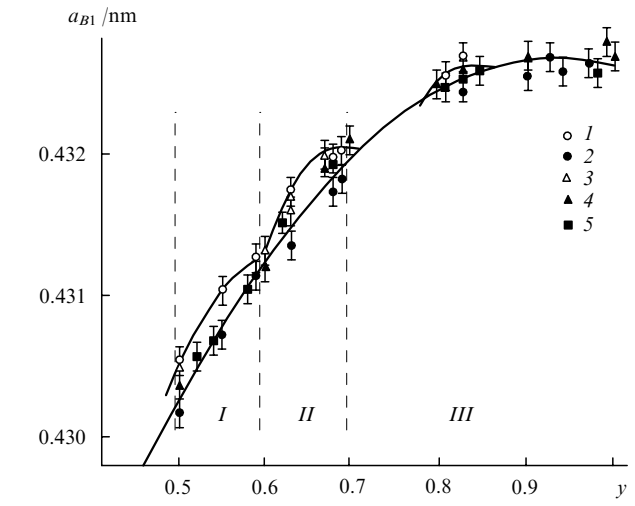


Figure 6. Lattice constant a_{B1} of the basic crystal lattice as a function of the composition of titanium carbide, TiC_y, in the quenched disordered (full circles) and annealed ordered (open circles) states.[57]
Samples obtained by sintering Ti and $TiC_{0.94}$ (*1*, *2*), by sintering Ti and C (*3*, *4*) and by hot pressing Ti and $TiC_{0.98}$ (*5*). The existence regions of the ordered phases Ti_2C, Ti_3C_2 and Ti_6C_5 are labelled I, II and III, respectively.

measured thermodynamic characteristics were attributed to a certain composition of the carbide with the known (disordered or ordered) structural state. The presence of the temperature and concentration dependences of thermodynamic characteristics of disordered carbide allows quantitative description of high-temperature phase equilibria involving TiC_y; however, of much greater importance is that using these data also provides the possibility of direct investigations into the disorder–order phase transformations. Unfortunately, the available experimental data on thermodynamic characteristics of nonstoichiometric titanium carbide are scarce.

b. Enthalpy (heat) of formation

Burning of a substance in oxygen in a calorimetric bomb is the main method of experimental determination of the formation enthalpy. Most of the data on the formation enthalpy of disordered TiC_y were obtained using this technique. The formation enthalpy can also be determined indirectly from the dependence of the partial pressure of the components of a compound on the evaporation temperature.

Calorimetric measurements of the standard formation enthalpy ($\Delta H^\circ_{f\,298}$) of titanium carbide of a nearly stoichiometric composition $TiC_{0.996}$ by burning of carbide in oxygen revealed [58] that $\Delta H^\circ_{f\,298} = -183.8 \pm 1.7$ kJ mol^{-1}. Calculations using the refined value of the formation enthalpy of titanium dioxide gave a more correct value: $\Delta H^\circ_{f\,298} = -184.6 \pm 1.7$ kJ mol^{-1}.[8]

Morozova *et al.*[59] determined the formation enthalpies of disordered cubic carbides of compositions $TiC_{0.79}$, $TiC_{0.91}$ and $TiC_{1.00}$ by burning them in oxygen and calorimetrically measuring the heat effect. The $\Delta H^\circ_{f\,298}$ values for these carbides were found to be -183.0 ± 2.1, -206.8 ± 0.8 and -192.6 ± 2.1 kJ mol^{-1}, respectively. The dependence of the formation enthalpy (in kJ mol^{-1}) determined by burning technique [59] on the composition of TiC_y can be described by the following formula:[1–3, 27]

$$\Delta H^\circ_{f\,298}(y) = -91.07 - 186.7\,y + 89.0\,y^2.$$

The formation enthalpies of carbides $TiC_{0.63}$, $TiC_{0.72}$, $TiC_{0.80}$ and $TiC_{0.91}$ (-108.0 ± 7.0, -135.0 ± 7.0, -157.0 ± 7.0 and -184.0 ± 7.0 kJ mol^{-1}, respectively) were determined from the data on vacuum evaporation of TiC_y in the temperature range from 1873 to 2673 K.[60, 61] The dependence of $\Delta H^\circ_{f\,298}$ (in kJ mol^{-1}) on the composition of TiC_y calculated using these values has the form [61]

$$\Delta H^\circ_{f\,298}(y) = 135.6 - 467.8\,y + 128.3\,y^2.$$

Comparison of the $\Delta H^\circ_{f\,298}(y)$ dependences obtained from calorimetric and evaporation measurements showed that these results are in satisfactory agreement for carbides with $y > 0.9$ but disagree at lower content of carbon. These dependences cannot be combined since the discrepancies between them seem to be due to the systematic errors of the methods employed. However, one can assume that the formation enthalpy of carbides TiC_y ($y < 0.9$) lies between the values found from calorimetric and evaporation measurements.

Analysis of the experimental data on the formation enthalpy of titanium monocarbide taking into account the position of the lower bound of the homogeneity region of TiC_y suggested [18] that the dependence of $\Delta H^\circ_{f\,298}$ (in kJ mol^{-1}) on the carbide composition has the form

$$\Delta H^\circ_{f\,298}(y) = 16.75 - 304.49\,y + 89.04\,y^2. \quad (1)$$

Mention may be made that dependence (1) is close to the average between the experimental dependences $\Delta H^\circ_{f\,298}(y)$ obtained from the results of calorimetric [59] and evaporation [61] measurements.

c. Enthalpy (heat content)

High-temperature enthalpy ($H^\circ_T - H^\circ_{298}$) measurements are usually carried out by a mixing technique using an adiabatic-shell calorimeter. The high-temperature enthalpy of titanium carbide was measured [62–65] and the following expressions for description of the temperature dependences of the enthalpy (in kJ mol^{-1}) were proposed.

For carbide of composition $TiC_{0.99}$ in the temperature range from 400 to 1800 K (see Ref. 62):

$$H^\circ_T - H^\circ_{298} = -19.95 + 49.53 \times 10^{-3} T + 1.67 \times 10^{-6} T^2 + 1499\,T^{-1}. \quad (2)$$

For carbide of composition $TiC_{0.95}$ (the measurement error was $\pm 1.4\%$) in the temperature range from 1300 to 2700 K (see Ref. 63)

$$H^\circ_T - H^\circ_{298} = -13.68 + 41.13 \times 10^{-3} T + 4.48 \times 10^{-6} T^2. \quad (3)$$

Storms [8] found the following formula for calculating the enthalpy (in kJ mol^{-1}) of stoichiometric compound $TiC_{1.0}$ in the temperature range from 300 to 3000 K

$$H^\circ_T - H^\circ_{298} = -22.19 + 55.67 \times 10^{-3} T - 4.07 \times 10^{-6} T^2 + 1763.6\,T^{-1} + 16.1 \times 10^{-10} T^3. \quad (4)$$

The enthalpies of disordered carbides $TiC_{0.64}$, $TiC_{0.71}$, $TiC_{0.82}$ and $TiC_{0.99}$ were measured in the temperature range 1300–2500 K by a mixing technique.[64,65] The authors suggested a polynomial description of the temperature dependence of the enthalpy; however, the polynomials did not fulfil the obvious normalisation condition:

$$H_T^\circ - H_{298}^\circ \equiv 0 \text{ at } T = 298\text{ K}.$$

Because of this, we calculated the temperature dependences of the enthalpy (in kJ mol^{-1}) of these carbides taking into account the normalisation condition[1,27] using the experimental data reported by Fesenko *et al.*[64] and the following expression

$$H_T^\circ - H_{298}^\circ = A + BT + CT^2 + DT^{-1}.$$

The corresponding formulae are as follows:
for carbide of composition $TiC_{0.64}$

$$H_T^\circ - H_{298}^\circ = -2.42 + 24.54\times10^{-3}T + 7.47\times10^{-6}T^2 - 1657.1\,T^{-1}, \quad (5)$$

for carbide of composition $TiC_{0.71}$

$$H_T^\circ - H_{298}^\circ = -2.03 + 24.46\times10^{-3}T + 8.12\times10^{-6}T^2 - 1780.9\,T^{-1}, \quad (6)$$

for carbide of composition $TiC_{0.82}$

$$H_T^\circ - H_{298}^\circ = -5.75 + 30.90\times10^{-3}T + 6.54\times10^{-6}T^2 - 1204.9\,T^{-1} \quad (7)$$

and for carbide of composition $TiC_{0.99}$

$$H_T^\circ - H_{298}^\circ = -12.97 + 36.61\times10^{-3}T + 6.79\times10^{-6}T^2 + 431.1\,T^{-1}. \quad (8)$$

These equations can be combined to derive a common function

$$(H_T^\circ - H_{298}^\circ)_{TiC_y} = \quad (9)$$
$$= (15.86 + 12.03\times10^{-3}T + 9.67\times10^{-6}T^2 - 6051.5\,T^{-1}) +$$
$$(-22.80 + 6.17\times10^{-3}T - 3.09\times10^{-6}T^2 + 6328.2\,T^{-1})\,y +$$
$$+ (-5.680 + 19.06\times10^{-3}T)\,y^2 \quad (\text{kJ mol}^{-1}),$$

which allows estimation of the enthalpy of disordered monocarbide TiC_y with any content of carbon in the temperature range from 300 to 2000 K.

d. Heat capacity and entropy

The heat capacity, C_p, of titanium carbides of compositions $TiC_{0.95}$ and $TiC_{0.99}$ was measured using the adiabatic technique in the temperature range from 12 to 300 K.[66] A decrease in the content of carbon in the TiC_y carbide is accompanied by a decrease in C_p. Lorenzelli *et al.*[67] measured the heat capacity of samples of disordered and ordered carbide of composition $TiC_{0.625}$ between 0.5 and 5.0 K; however, they presented only the difference between the heat capacities of the samples.

Since

$$C_p = \frac{\mathrm{d}(H_T^\circ - H_{298}^\circ)}{\mathrm{d}T},$$

the high-temperature heat capacity is usually determined using the results of experimental enthalpy measurements. This allows the functions (5)–(9) to be used for estimating the heat capacity of disordered TiC_y.

The entropy, S_{298}°, of stoichiometric titanium monocarbide $TiC_{1.0}$ is 24.24 J mol^{-1} K^{-1} (see Ref. 8). No experimental data on changes in entropy within the homogeneity region of cubic carbide TiC_y are available so far. To a first approximation, the dependence of entropy on the composition of carbide MC_y can be represented by the additive sum of the entropies of the components normalised to the entropy of stoichiometric carbide $MC_{1.0}$, *i.e.*,

$$S_{298}^\circ(y) = k(S_{298\,M}^\circ + yS_{298\,C}^\circ), \quad (10)$$

where $k = S_{298\,MC_{1.0}}^\circ/(S_{298\,M}^\circ + S_{298\,C}^\circ)$ is the normalisation constant and $S_{298\,M}^\circ$ and $S_{298\,C}^\circ$ are the entropies of the metal and carbon, respectively. The entropies of α-Ti and carbon are 30.72 (see Ref. 68) and 5.39 J mol^{-1} K^{-1} (see Ref. 69), respectively. Taking into account these values and the value $S_{298\,TiC_{1.0}}^\circ = 24.24$ J mol^{-1} K^{-1} (see Ref. 8), the normalisation constant, k, was found to be 0.671. To a first approximation, the dependence of entropy (in kJ mol^{-1} K^{-1}) on the composition, TiC_y, has the form

$$S_{298}^\circ(y) = 20.62 + 3.62\,y. \quad (11)$$

e. The free energy

The free energy of disordered carbide can be calculated using the dependences (1), (9) and (11).

Indeed, thermodynamic properties of solids are usually described assuming a constant pressure (usually, p is set to 0 or 1). Under isobaric conditions, the internal energy (configuration energy of a crystal), E, equals the enthalpy H. At 298 K, the enthalpy of a compound is equal to the formation enthalpy of this compound from corresponding elements, *i.e.*, $H_{298}^\circ \equiv \Delta H_{f298}^\circ$. Taking into account the temperature dependence of the enthalpy of nonstoichiometric compound MX_y, from here it follows that

$$E(y,T) = H(y,T) = H_{298}^\circ(y) + (H_T^\circ - H_{298}^\circ)_{MX_y} \equiv \quad (12)$$
$$\equiv \Delta H_{f298}^\circ(y) + (H_T^\circ - H_{298}^\circ)_{MX_y}.$$

The free energy (F) of a disordered nonstoichiometric compound MX_y is given by the following expression[1–3,14,17,20,22,70]

$$F(y,0,T) = E(y,T) - T[S(y,0,T) + S_c(y,0)] \equiv \quad (13)$$
$$\equiv F_0(T) + yF_1(T) + y^2F_2(T) - TS_c(y,0),$$

where $S(y,0,T)$ is the non-configurational entropy, which is an explicit function of temperature; $S_c(y,0)$ is the combinatorial (configurational) entropy, which is independent of temperature; and $F_0(T)$, $F_1(T)$ and $F_2(T)$ are the free energy parameters.

Using the standard entropy, the temperature dependence of entropy can be written as follows

$$S(T) = S_{298}^\circ + \int_{298}^{T} \frac{\mathrm{d}(H_T^\circ - H_{298}^\circ)}{T}.$$

In this case

$$S(y,0,T) = S_{298}^\circ(y) + \int_{298}^{T} \frac{\mathrm{d}(H_T^\circ - H_{298}^\circ)_{MX_y}}{T}. \quad (14)$$

The free energy of a disordered compound MX_y minus the term responsible for the contribution of configuration entropy, $S_c(y,0)$, is given by the expression

$$F_0(T) + yF_1(T) + y^2F_2(T) \equiv E(y,T) - TS(y,0,T) \quad (15)$$

or, taking into account Eqns (12) and (14),

$$F_0(T) + yF_1(T) + y^2F_2(T) = \Delta H_{f298}^\circ(y) + \quad (16)$$
$$+ (H_T^\circ - H_{298}^\circ)_{MX_y} - T\left[S_{298}^\circ(y) + \int_{298}^{T} \frac{\mathrm{d}(H_T^\circ - H_{298}^\circ)_{MX_y}}{T}\right].$$

The expression for a fraction of the free energy (in kJ mol^{-1}) of disordered carbide TiC_y was derived[1–3,27] from Eqn (16) using the dependences (1), (9) and (11)

$$F_0(T) + yF_1(T) + y^2F_2(T) = \quad (17)$$
$$= (32.61 + 31.61\times10^{-3}T - 9.67\times10^{-6}T^2 - 3026T^{-1} -$$
$$- 12.03\times10^{-3}T\ln T) + (-327.29 + 71.49\times10^{-3}T +$$
$$+ 3.09\times10^{-6}T^2 + 3164T^{-1} - 6.17\times10^{-3}T\ln T)y +$$
$$+ (83.36 + 127.65\times10^{-3}T - 19.06\times10^{-3}T\ln T)y^2,$$

where the parameters $F_0(T)$, $F_1(T)$ and $F_2(T)$ of the free energy $F(y,0,T)$ [see Eqn (13)] are given in explicit form. Knowledge of these parameters allows all types of thermodynamic calculations of the phase equilibria involving nonstoichiometric titanium carbide.

3. High-temperature evaporation of titanium carbide

Thermodynamic properties of nonstoichiometric carbides are often determined using measurements of the vapour pressure above the solid compounds. Of particular interest is the case of congruent evaporation.

According to the kinetic theory of gases, the rate of evaporation from the surface that is in equilibrium with vapour equals the condensation rate, which is proportional to the equilibrium vapour pressure p. Under nonequilibrium conditions (in the case of, *e.g.*, vacuum evaporation from the open surface) the evaporation rate is independent of the condensation rate and equals the equilibrium evaporation rate at a given temperature;[71] this holds if the residual pressure in the vacuum chamber does not exceed 10 Pa. Therefore, knowledge of the rate of steady-state vacuum evaporation allows determination of the equilibrium parameter, namely, the saturated vapour pressure, and calculation of the thermodynamic characteristics. If transition from the condensed phase to the vapour phase is accompanied by dissociation of the former, the observed evaporation rate and the partial pressure are lower than the equilibrium values; this can be taken into account by introducing the evaporation coefficient $\alpha \leqslant 1.0$.

The kinetic and thermodynamic conditions for congruent evaporation of disordered nonstoichiometric interstitial compounds have been studied in detail in monograph.[14] Thermodynamics of congruent evaporation of nonstoichiometric compounds was also developed.[72, 73].

Evaporation of TiC_y at temperatures above 1800 K was studied by many authors. Mass spectrometric studies of the composition and the pressure measurements of the vapour above titanium carbide evaporated from a graphite effusion chamber (evaporation in the presence of excess of free carbon) at 2200–2500 K showed that the vapours contained elemental carbon and titanium and the C_2 and C_3 units; no molecular species TiC were found.[74, 75] The vapour pressure of titanium above the titanium carbide–graphite system at 2383–2593 K measured [76] by the Knudsen effusion technique was found to be much higher than that determined by other authors. The value reported in this study seems to be overestimated, since evaporation of pure graphite through the effusion orifice was ignored. In the temperature range between 2518 and 2790 K, the vapours above the titanium carbide–carbon system contained Ti, TiC_2, TiC_4 and C_3 units.[77] According to estimates,[78] the gas phase above this system contains elemental titanium and carbon as the major components at $T < 2500$ K and Ti, C and C_3 units at $T > 2500$ K. Titanium carbide was shown to undergo dissociation during evaporation at $2200 < T \leqslant 2500$ K in the presence of excess of free carbon; in this case, elemental titanium is released in the gaseous state while carbon is released in the solid state.[74–76]

Studies of evaporation of carbide $TiC_{0.97}$ at 2773 K using Langmuir's technique revealed that under these conditions the compound undergoes congruent evaporation and that the vapours contain mostly elemental titanium and carbon.[79] The composition of carbide TiC_y affects the vapour pressure, namely, the vapour pressure of titanium monotonically increases from 1×10^{-4} Pa for $TiC_{0.91}$ to 0.2 Pa for $TiC_{0.55}$ as the content of carbon decreases (see Ref. 8). Evaporation and dissociation of carbide $TiC_{0.91}$ in the temperature range between 1873 and 2673 K can be described by the reaction [80]

$$TiC_y\,(s) \longrightarrow Ti\,(g) + [y - z(T)]C\,(g) + z(T)C\,(s), \quad (18)$$

where $z(T) = y$ at $T \leqslant 2100$ K; $z(T)$ decreases from y down to 0 as the temperature increases from 2100 to 2273 K; $z(T) = 0$ at $T \geqslant 2273$ K. The vapour pressure of titanium above carbide $TiC_{0.91}$ at 1900 K was found to be $\sim6\times10^{-5}$ Pa,[80] which is close to the value reported by Storms.[8]

Evaporation of titanium carbide was mainly studied near the upper bound of the homogeneity region of the cubic phase taking the TiC_y samples with $y > 0.9$ as examples (see Refs 74–77, 79 and 80). The evaporation coefficient was assumed to be equal to unity, though if evaporation is accompanied by dissociation, this value is less than 1. The results of determination of the vapour pressure of titanium reported by different authors [8, 74–77, 79, 80] are substantially different (from 2 to 40 times).

Vacuum evaporation (at 0.0013 Pa) of samples of cubic monocarbide TiC_y with different contents of carbon ($0.6 < y \leqslant 0.93$) was studied in the temperature range between 1873 and 2673 K.[60, 61] The samples represented disordered titanium carbide, since only disordered nonstoichiometric carbides are in thermodynamic equilibrium at $T > 1300$–1500 K.[1–3, 14, 17, 70] All TiC_y samples were found to be homogeneous and contained one phase with the $B1$-type structure. Evaporation of titanium carbide was studied by Langmuir's technique. The evaporation rate

$$V = \frac{\Delta m}{S_{ef}\,t}$$

was determined from the mass loss (Δm) from the effective evaporation surface area, S_{ef}, of a vacuum heated sample over a period t. Due to the presence of the open surface pores the S_{ef} value was larger than the geometric evaporation surface area S

$$S_{ef} = S\left[1 + \left(\frac{9\pi P^2}{2}\right)^{1/3}\right],$$

where P is the relative porosity. The evaporation surface area was determined [60, 61] with allowance for porosity which was determined as the average between the initial (before the experiment) and final (after heating) porosity. Evaporation was carried out until establishment of a constant total evaporation rate V (for a given temperature) and a constant crystal lattice parameter on the surface of the sample, *i.e.*, until steady-state regime of the process.

The overall time of vacuum evaporation of titanium carbide samples varied from 2–8 h at 2673 K to 54 h at 1873 K. During evaporation the lattice constant on the surface of the samples remained virtually unchanged, which indicated a constant composition of TiC_y at $T < 2673$ K.

Evaporation of carbides TiC_y at $T < 2273$ K led to release of elemental carbon on the surface of the samples, whereas no elemental carbon was found on the surface of the TiC_y samples at higher evaporation temperatures ($T \geqslant 2273$ K). These data and the results of evaporation rate measurements suggest that at $T \leqslant 2273$ K evaporation of titanium carbide TiC_y is described by reaction (18). Indeed, at $T < 2100$ K the pressure and evaporation rate of metallic titanium are much higher than those of elemental carbon;[68] because of this, carbon is mainly released in the solid phase and can thus be found on the surface of the samples. As the content of carbon in TiC_y decreases (especially at $y \leqslant 0.8$), the amount of elemental carbon released on the surface rapidly decreases. Raising the temperature leads to an increase in the evaporation rate of carbon and no elemental carbon was found on the surface of TiC_y samples at $T > 2300$ K. At $T > 2273$ K, which corresponds to complete evaporation of carbon released on the surface, the $z(T)$ value equals zero, and the equilibrium in system (18) loses ambiguity. Since at temperatures below 2600 K (in the absence of excess elemental carbon) the vapour above titanium carbide contains mostly elemental

Table 3. Total evaporation rate V (kg m^{-2} s^{-1}) and partial pressure p°_{Ti} (Pa) in the temperature range between 2273 and 2673 K, evaporation coefficients α_{Ti} and α_C, atomisation enthalpy ($\Delta_{at}H^{\circ}_{298}$ /kJ mol^{-1}), formation enthalpy ($\Delta H^{\circ}_{f\,298}$ / kJ mol^{-1}) and evaporation enthalpy ($\Delta_s H^{\circ}_{298}$ /kJ mol^{-1}) of TiC_y samples.[61]

TiC_y	$\ln V = a - b/T$		α_{Ti}	α_C	$\ln p^{\circ}_{Ti} = a - b/T$ (see [a])		$\Delta_{at}H^{\circ}_{298}$		$\Delta H^{\circ}_{f\,298}$	$\Delta_s H^{\circ}_{298}$
	a	*b*			*a*	*b*	see [b]	see [c]		
$TiC_{0.63}$	21.545 ± 0.091	72609 ± 225	0.80 ± 0.05	0.40 ± 0.05	29.538 ± 0.084	73836 ± 209	1028 ± 2	1025 ± 2	−108 ± 7	553 ± 70
$TiC_{0.72}$	21.882 ± 0.034	75111 ± 85	0.90 ± 0.05	0.45 ± 0.05	29.721 ± 0.035	76339 ± 87	1119 ± 2	1115 ± 2	−135 ± 7	644 ± 70
$TiC_{0.80}$	21.998 ± 0.129	77011 ± 322	0.90 ± 0.10	0.45 ± 0.10	29.987 ± 0.170	78601 ± 423	1198 ± 6	1193 ± 4	−157 ± 7	723 ± 70
$TiC_{0.91}$	21.700 ± 0.027	79115 ± 67	0.60 ± 0.05	0.30 ± 0.05	29.921 ± 0.023	80342 ± 57	1303 ± 1	1299 ± 1	−184 ± 7	828 ± 70

[a] For carbide TiC_y, $\ln p^{\circ}_C = \ln p^{\circ}_{Ti} + \ln y$. [b] Found using the equation of the second law of thermodynamics (see below). [c] Found using the equation of the third law of thermodynamics (see below).

titanium and carbon and does not contain C_2 units and larger carbon molecular species and titanium carbide molecules,[78] one can suggest congruent evaporation of TiC_y in the temperature range between 2273 and 2673 K following the reaction

$$TiC_y\ (s) \longrightarrow Ti\ (g) + y\,C\ (g). \qquad (19)$$

This character of evaporation of TiC_y has been confirmed experimentally.[78–80]

An increase in the evaporation temperature causes a rapid increase in the evaporation rate: *e.g.*, the evaporation rate of $TiC_{0.92}$ increases by a factor of more than 20 000 as the temperature increases from 1873 to 2673 K. For TiC_y samples with different contents of carbon the temperature dependence of the evaporation rate has the form

$$\ln V = a - \frac{b}{T}.$$

In Table 3 we present the values of the coefficients a and b for some carbides. The evaporation rate of carbide of composition $TiC_{0.92}$ calculated using this dependence for 2773 K is 108×10^{-5} kg m^{-2} s^{-1}. This is rather close to the estimate $(93-113) \times 10^{-5}$ kg m^{-2} s^{-1} for the evaporation rate of $TiC_{0.97}$ at 2773 K.[79]

If a compound MC_y undergoes congruent evaporation, the observed partial pressures of its components, p_M and p_C, are [14, 71, 80]

$$p_M = \alpha_M p^{\circ}_M = \frac{V(2\pi RTA_M)^{1/2}}{M}, \qquad (20)$$

$$p_C = \alpha_C p^{\circ}_C = \frac{yV(2\pi RTA_C)^{1/2}}{M}, \qquad (21)$$

where α_M, α_C and p°_M, p°_C are the evaporation coefficients and the equilibrium partial pressures of the metal and non-metal components of condensed carbide MC_y; V is the total evaporation rate; A_M and A_C are the atomic masses of the metal and carbon, respectively, and $M = A_M + yA_C$ is the molecular mass of carbide MC_y.

Under equilibrium congruent evaporation one gets $p^{\circ}_C = y\,p^{\circ}_M$; hence from Eqns (20) and (21) it follows [14] that

$$\alpha_C = \alpha_M \left(\frac{A_C}{A_M}\right)^{1/2},$$

$$p_C = y\left(\frac{A_C}{A_M}\right)^{1/2} p_M.$$

In Fig. 7 we present the dependences of the partial pressure of titanium on the composition of carbide TiC_y. At any temperature, the larger the deviation of the carbide composition from the stoichiometric composition, the higher the p_{Ti} value. Earlier, an analogous type of change in p_{Ti} was reported for $T = 1900$ K.[8]

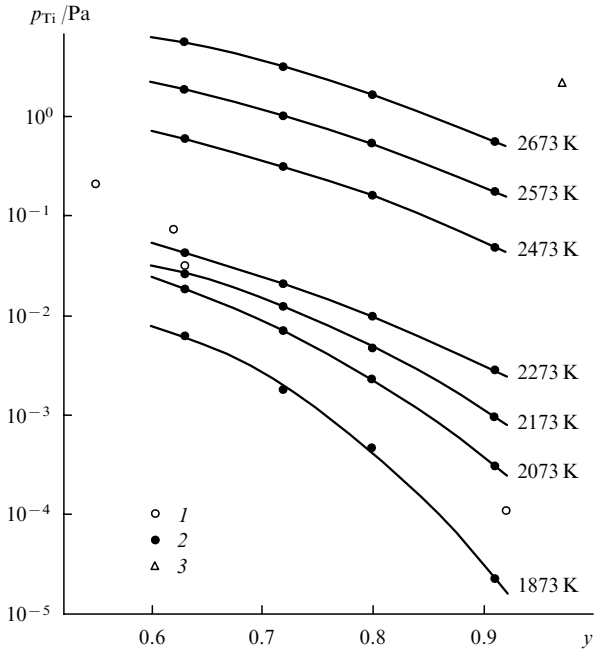


Figure 7. Partial pressure of titanium, p_{Ti}, as a function of the composition of titanium carbide, TiC_y,: pressure p_{Ti} above the TiC_y carbide at 1900 K (*1*);[8] data [61] (*1*) and pressure p_{Ti} above the $TiC_{0.97}$ carbide at 2773 K (*3*).[79]

Taking into account the relationship

$$p_C = y\left(\frac{A_C}{A_M}\right)^{1/2} p_M,$$

the equilibrium constant, K, of reaction (19) is (when calculating K values, the partial pressure is given in atmospheres):

$$K = p_M p_C = p_M^{(1+y)} y y \left(\frac{A_C}{A_M}\right)^{y/2} = \alpha_M^{(1+y)} (p^{\circ}_M)^{(1+y)} y^y \left(\frac{A_C}{A_M}\right)^{y/2}. \qquad (22)$$

Knowledge of the equilibrium constant K allowed estimation of the enthalpy of process (19);[61] in the case of evaporation accompanied by dissociation this is the atomisation enthalpy $\Delta_{at}H^{\circ}_{298}$. In accord with the second law of thermodynamics, the $\Delta_{at}H^{\circ}_{298}$ value was found using the available temperature dependences of K and by solving Van't Hoff's isobar equation

$$\frac{d\ln K}{dT} = \frac{\Delta_{at}H^{\circ}_T}{RT^2}. \qquad (23)$$

Calculations of $\Delta_{at}H^{\circ}_{298}$ were carried out with inclusion of correction Δ for the temperature dependence of the enthalpy of the components of reaction (19):

$$\Delta = (H_T^\circ - H_{298}^\circ)_{\mathrm{Ti(g)}} + y(H_T^\circ - H_{298}^\circ)_{\mathrm{C(g)}} -$$

$$- (H_T^\circ - H_{298}^\circ)_{\mathrm{TiC}y\mathrm{(s)}}.$$

The $\Delta_{at}H_{298}^\circ$ values for carbides TiC_y under study were found by the least-squares minimisation of the expression

$$R\ln K(T) = c - \frac{\Delta_{at}H_{298}^\circ + \Delta}{T},$$

where c is a constant, using the experimental dependences $K(T)$. The heat effect of reaction (19), *i.e.*, the atomisation enthalpy of carbide TiC_y, was also determined using the equation of the third law of thermodynamics.

$$\Delta_{at}H_{298}^\circ = T\Delta\Phi'_T - RT\ln K$$

with allowance for the calculated temperature and concentration dependence of the reduced potential $\Delta\Phi'_T$.

The calculated standard atomisation enthalpies, $\Delta_{at}H_{298}^\circ$, of titanium carbides of different composition and the evaporation coefficients α_M and α_C are listed in Table 3. The parameters of the dependences $\ln V - T$ and $\ln p_{Ti}^\circ - T$ (see Table 3) correspond to the temperature range of congruent evaporation of TiC_y (from 2273 to 2673 K).

The dependence of the atomisation enthalpy on the composition of carbide TiC_y calculated by the least squares method using the $\Delta_{at}H_{298}^\circ$ values calculated from the equations of the second and third laws of thermodynamics has the form:

$$\Delta_{at}H_{298}^\circ(y)_{\mathrm{TiCy}} = 335.4 + 1177.8\,y - 128.3\,y^2 \pm 7. \qquad (24)$$

For compounds MX_y, the atomisation enthalpy is given by the expression

$$\Delta_{at}H_{298}^\circ(y) = \Delta_s H_M^\circ + y\Delta_s H_X^\circ - \Delta H_{f298}^\circ(y), \qquad (25)$$

where $\Delta_s H_M^\circ$ and $\Delta_s H_X^\circ$ are the evaporation enthalpies of the components M and X, respectively, and $\Delta H_{f298}^\circ(y)$ is the formation enthalpy of compound MX_y. The expression for the dependence of the heat of formation of carbide TiC_y on its composition derived using the relationships (24) and (25) and the reference data on the evaporation enthalpies of titanium and carbon, $\Delta_s H_{Ti}^\circ = 471$ and $\Delta_s H_C^\circ = 710$ kJ mol^{-1} (see Ref. 68) has the form [60, 61]

$$\Delta H_{f298}^\circ(y)_{\mathrm{TiC}_y} = 135.6 - 467.8\,y + 128.3\,y^2 \pm 7. \qquad (26)$$

The $\Delta H_{f\,298}^\circ$ values for carbides of compositions $TiC_{0.79}$, $TiC_{0.91}$ and $TiC_{1.00}$ were found to be -157, -184 and -204 kJ mol^{-1}, respectively;[61] this is in fairly good agreement with the results of earlier studies [*cf.* the $\Delta H_{f\,298}^\circ$ values of -183, -207 (see Ref. 59) and -184 kJ mol^{-1} (see Ref. 58) for carbides of compositions $TiC_{0.79}$, $TiC_{0.91}$ and $TiC_{0.996}$, respectively]. The dissociation enthalpy of a gaseous titanium carbide molecule is 473 ± 60 kJ mol^{-1} (see Refs 68, 81). Using this value, the evaporation enthalpy of titanium carbide TiC_y was also roughly estimated [60, 61] as the difference between the atomisation and dissociation enthalpies (see Table. 3).

4. Nanocrystalline titanium carbide

Establishment of the fact that reduction of the grain or crystallite size down to and below a certain threshold value can cause substantial changes in the properties of solids[82–86] gave a strong impetus to investigations of the nanocrystalline state of matter. Pioneering studies in this field were reported by Gleiter [87–90] who developed a method for fabrication of compact nanomaterials from nanopowders (the so-called 'compaction'). Ultradispersed and nanocrystalline transition metal carbides can be prepared by plasmachemical synthesis, mechanochemical synthesis, intense plastic deformation and structure ordering.[91, 92] Investigations of the nanocrystalline state of carbides are directed at making them less brittle and at improving their plasticity with simultaneous retention of high hardness typical of these compounds.

Ultradispersed transition-metal carbide powders are usually obtained by the interaction of chlorides of corresponding elements with dihydrogen and methane or other hydrocarbons in the low-temperature (4000 – 8000 K) argon plasma. The particles of such powders are single crystals 10 to 100 – 200 nm in size. Finely dispersed titanium, zirconium, niobium, tantalum, boron and silicon carbide powders were prepared by a plasmachemical technique.[93, 94]

Gas-phase synthesis involving laser heating of the mixture of reactant gases is a kind of plasmachemical synthesis.[95–98] Laser heating allows control of homogeneous nucleation and excludes contamination. As the intensity of laser radiation increases, the size of nanoparticles decreases due to an increase in the temperature and in the heating rate of the reactant gases.

In the last decade, a mechanochemical technique has found wide use for the synthesis of nanocrystalline carbides. Mechanical milling is the most efficient method for production of large amounts of powders of different nanomaterials including carbides. Mechanochemical synthesis of nanocrystalline titanium carbide from a mixture of the metal and carbon powders was reported.[99] The mixture was ball milled. Formation of carbide occurred after pulverisation over a period of 4 to 12 h; the average particle size of the nanocrystalline powder after 48 h milling was 7 ± 1 nm.

Nanocrystalline powder of cubic titanium carbide was also prepared by pulverising metallic titanium and graphite in a sapphire ball mill. The components were taken in a ratio that provided a $Ti_{44}C_{56}$ composition of the product.[100] The ball-to-powder mass ratio was 10 : 1. Milling was performed at room temperature in an argon atmosphere.

After pulverisation for 2000 s the X-ray diffraction pattern of the reactant mixture exhibited only broad reflections of elemental carbon and titanium (Fig. 8). Milling over a period of 1.1×10^4 s led to nearly complete disappearance of the graphite reflections. New reflections appeared after pulverisation for 1.5×10^4 s corresponded to a new cubic phase with the $B1$-type structure, *viz.*, titanium carbide. The lattice constant of titanium carbide pre-

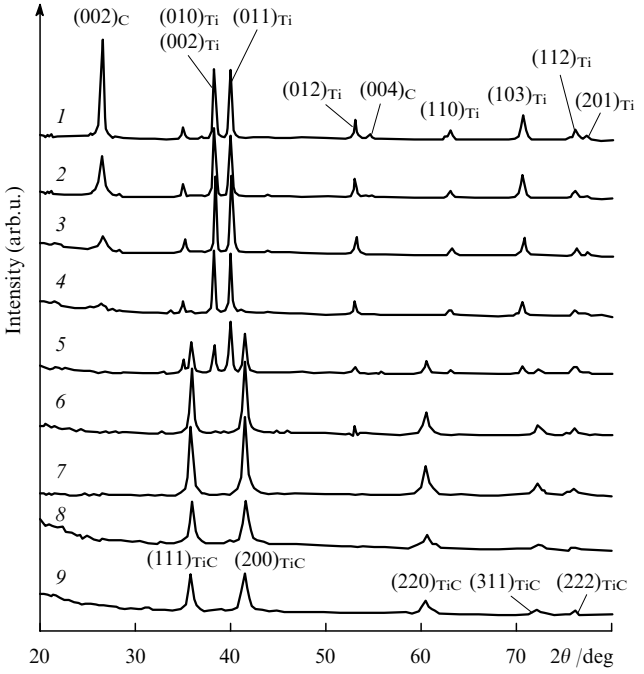


Figure 8. Changes in the X-ray diffraction patterns of a powder mixture $Ti_{44}C_{56}$ as a function of milling duration (t) in the mechanochemical synthesis of titanium carbide ($CuK_{\alpha 1,2}$ radiation).[100]
$t = 2 \times 10^3$ (*1*), 6×10^3 (*2*), 8×10^3 (*3*), 1.15×10^4 (*4*), 1.5×10^4 (*5*), 2.2×10^4 (*6*), 4×10^4 (*7*), 8×10^4 (*8*) and 7.2×10^5 s (*9*).

pared in this manner was 0.4326 nm. Prolonged milling (4×10^4 s) led to complete disappearance of the reflections of metallic titanium and to an increase in the intensity of titanium carbide reflections. After 8×10^4 s, mechanical deformation of the powder particles developed and the grain size reduced dramatically, which was manifested in substantial broadening of reflections in the X-ray diffraction pattern. Pulverisation for 72×10^4 s resulted in the formation of titanium carbide nanocrystals. No observable changes in the state of the carbide sample were detected upon further extension of milling duration to 10^6 s.

Figure 9 illustrates the changes in the powder grain size during pulverisation according to X-ray diffraction and electron microscopy studies. The formation of nanocrystalline titanium carbide involves four stages. The first stage (milling for no longer than 1.1×10^4 s) is characterised by the formation of Ti/C composite particles with an average size of ~ 1000 nm. Metallographic tests revealed an onion-like structure of these species comprised of titanium and carbon layers. In the second stage, which takes from 1.1×10^4 to 2×10^4 s, solid-phase interaction between titanium and carbon occurs, resulting in coarse-grained titanium carbide particles 800 to 1000 nm in size. The third stage takes from 2×10^4 to 8×10^4 s and involves intense milling of titanium carbide grains followed by the formation of finely dispersed powder with a rather broad grain size distribution (from 5 to 100 nm in diameter); in this stage, titanium carbide grains form agglomerates of size 5 to 10 μm. The last, fourth, stage takes 8×10^4 to 1×10^6 s and is characterised by 'grain size homogenisation' of the nanocrystalline powder. Carbide powder thus obtained had a particle size of $\sim 2 \pm 1$ nm while its grains were agglomerated into spherulites of size no greater than 300 nm.

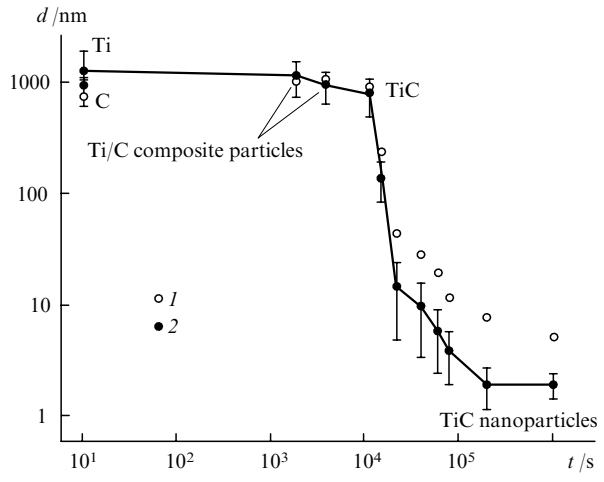


Figure 9. Grain size (d) of milled $Ti_{44}C_{56}$ powder as a function of milling duration t in the mechanochemical synthesis of titanium carbide.[100]
The grain size was determined from broadening of X-ray diffraction reflections (*1*) and by electron microscopy (*2*).

Titanium carbide powders prepared [100] by milling over different periods of time (2.2×10^4, 4×10^4, 8×10^4 and 7.2×10^5 s) were sintered in activated plasma. This type of sintering is a kind of hot pressing. Salient features of the method are the use of pulsed voltage for plasma activation and combination of nonaxial torsion with pressure. Sintering for less than 8 min resulted in compact titanium carbide samples of high density (up to 5.2 g cm^{-3}) while the average grain size remained less than 70 nm. The microhardness of the sintered samples (32 ± 3 GPa) was no greater than that of conventional coarse-grained titanium carbide TiC_y ($0.9 \leqslant y \leqslant 1.0$).

The results obtained by El-Eskandarany *et al.*[100] pointed to high efficiency of mechanochemical synthesis for fabrication of nanocrystalline titanium carbide; however, no data on the chemical composition of the carbide were reported in this study. The assumption [100] that the composition of mechanochemically synthesised titanium carbide is identical to that of the initial mixture ($Ti_{44}C_{56}$) seems to be doubtful. The reported lattice constant of titanium carbide is somewhat smaller, while the measured density is higher than the corresponding parameters of stoichiometric carbide $TiC_{1.0}$ (0.4328 nm and 4.91 g cm^{-3}, respectively). The reason for such a high density of titanium carbide obtained by El-Eskandarany *et al.*[100] is particularly incomprehensible. Even assuming that the synthesised carbide with the $B1$-type structure has the same composition as the charge [*i.e.*, $Ti_{0.44}C_{0.56}$ (or $TiC_{1.27}$!?)], the metal sublattice of this carbide should contain defects, since for the $B1$-type structure the number of sites in the non-metal sublattice is the same as that in the metal sublattice and there are no possibilities of arranging any sort of excess atoms. If a particular sort of atom is in relative excess, the sublattice formed by the other sort of atom contains structural vacancies. In our case titanium carbide with the defect metal sublattice can have a composition $Ti_{0.79}C_{1.00}$; however, its density should be 20% lower than the calculated (theoretical) value. Noteworthy is that no vacancies were found so far in the metal sublattice of carbides; therefore, the metal sublattice of transition metal carbides is assumed to be perfect. Taking into account the aforesaid, the results obtained by El-Eskandarany *et al.*[100] should be thoroughly checked. We believe that titanium carbide synthesised in that study was highly contaminated with metal, which led to higher density of the material compared to the theoretical value.

A promising way of producing compact nanomaterials is to employ intense plastic deformation.[85, 92, 101] Preparation of compact samples of nanocrystalline titanium carbide using this technique was reported.[102] Milling and compacting experiments were carried out with coarse-grained ($d \approx 2-5$ μm) powder of nonstoichiometric carbide $TiC_{0.62}$. Intense plastic deformation was produced by applying torsion under quasi-hydrostatic pressure. X-Ray diffraction studies revealed retention of the $B1$-type cubic structure of all plastic deformed titanium carbide samples; however, the diffraction reflections were substantially broadened (Fig. 10). Evaluation of the grain size from the broadening magnitude showed that the compacted nanocrystalline samples of nonstoichiometric titanium carbide had an average grain size lying between ~ 30 and 50 nm. Contrary to metals, titanium carbide is very hard and brittle; therefore, it is of considerable interest that the grain size of titanium carbide was smaller than that of the metal samples after nearly identical plastic deformation.

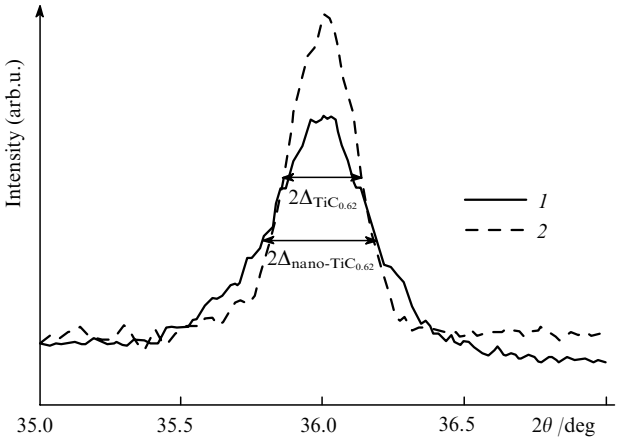


Figure 10. Broadening of the $(111)_{B1}$ reflection of nanocrystalline titanium carbide of composition $TiC_{0.62}$ prepared by intense plastic deformation (*1*) and coarse-grained (grain size ~ 5 μm) carbide $TiC_{0.62}$ (*2*).[102]
2Δ is the total width of the reflection at half-maximum ($CuK_{\alpha 1,2}$ radiation).

III. New chemical compounds in the Ti – C system

The discovery of molecular clusters of carbon and the first observations of the C_{60} fullerene molecule [103–105] gave an impetus to investigations into the synthesis, structure and properties of fullerenes (see, *e.g.*, Refs 106–108) and to an intensive search for methods of obtaining molecular clusters of other substances. By analogy with fullerenes, molecular clusters were expected to have unique physical and chemical properties that differ from the properties of the known polymorphous modifications of the same substances.

1. Molecular cluster Ti_8C_{12}

In 1992,[28] search for new molecular clusters led to the discovery of unusual, stable charged cluster $Ti_8C_{12}^+$ corresponding to a pentagondodecahedral molecule of stoichiometric composition Ti_8C_{12} (Fig. 11 *a*). In an ideal dodecahedral molecule, all atoms are arranged on a sphere whose surface is obtained by linking adjacent atoms and comprises twelve regular pentagons. In this molecule, all carbon and titanium atoms are tricoordinated (similarly to fullerene C_{60}), occupy identical sites and are distributed over the vertices of the dodecahedron in such a manner that the Ti atom is linked to carbon atoms only while six C_2 units alternate with eight Ti atoms. The dodecahedral structure of Ti_8C_{12} can be represented as a cube with eight titanium atoms at the vertices and a C_2 unit in each face. The point symmetry group, T_h, of this structure includes 24 symmetry elements (rotations and reflections). High symmetry of the met-car (metallocarbohedrene) molecule implies its stability.

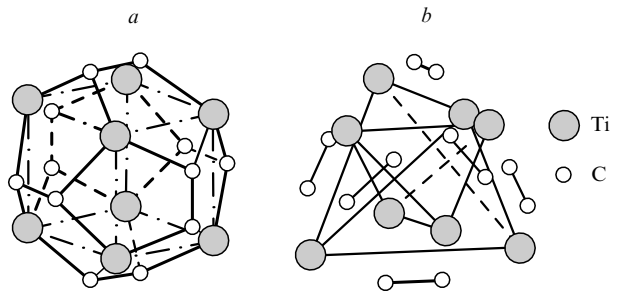


Figure 11. Dodecahedral structure of a Ti_8C_{12} molecular cluster of T_h symmetry (*a*) and a fragment of structure of T_d symmetry (*b*).[29]

Yet another possible structure of the Ti_8C_{12} cluster is characterised by the point symmetry group T_d (see Fig. 11 *b*).[29] In this structure, titanium atoms occupy two types of lattice sites and each type of site forms a tetrahedron. The smaller tetrahedron is rotated by 90° about the larger tetrahedron. The sites in the titanium sublattice differ in arrangement with respect to the C_2 units. Indeed, six C_2 units are arranged parallel to the edges of the larger tetrahedron built of Ti(1) atoms and perpendicular to the edges of the smaller tetrahedron formed by four Ti(2) atoms. The Ti(1) atoms are linked to three adjacent carbon atoms while the Ti(2) atoms form bonds with six carbon atoms. The Ti(1)–C and Ti(2)–C distances are 0.193 and 0.219 nm, respectively.[29]

The issue of which structural type is practically realised is still to be clarified since no molecular crystals of met-cars have been synthesised so far.

Clusters Ti_8C_{12} were synthesised using the gas-phase plasma-chemical technique with helium as inert gas, hydrocarbons (methane, ethylene, acetylene, propylene and benzene) and titanium vapours as reactants; the pressure of the gas mixture in the reactor was 93 Pa. A rotating metallic titanium rod was evaporated by exposing it to focussed radiation of a Nd laser operated at 532 nm, thus creating an ionised metal vapour beam. Neutral and ionised clusters were separated from other reaction products and analysed mass spectrometrically. The mass spectra of the reaction products exhibited a sharp peak corresponding to the Ti_8C_{12} molecule. In addition to neutral molecules, the mixture of ionised gases also contained stable $Ti_8C_{12}^+$ ions.

The cluster Ti_8C_{12} was assumed[28] to be a member of a novel class of molecular clusters and called metallocarbohedrene or met-car (see Ref. 106). In met-cars, both the transition metal and carbon atoms form a cage-like structure. Indeed, other M_8C_{12} clusters of such transition metals as Zr, Hf, V,[30,31] Cr, Mo and Fe[32] were obtained after a short time. Met-cars have been reviewed.[33,34]

The high stability of the cluster Ti_8C_{12} is thought to be due to peculiarities of its molecular and electronic structure; chemical bonds in the Ti_8C_{12} molecule are similar to those in the carbon fullerenes.[28] However, in contrast to C_{60} fullerene, both ionised and neutral M_8C_{12} molecules are comprised of five-membered rings only. The shape of the surface of stable cluster Ti_8C_{12} is similar to that of hypothetical unstable (and, hence, unfeasible) C_{20} fullerene. This fact shows that full similarity of chemical bonds in the clusters M_8C_{12} to those in carbon fullerene is hardly probable.

Indeed, calculations of the equilibrium crystal and electronic structure of the cluster Ti_8C_{12} with T_h symmetry (see Ref. 35) showed that the bonds between the titanium atoms and three adjacent carbon atoms differ from the bonds between carbon atoms in graphite or C_{60} fullerene. In particular, the Ti–C and C–C bond lengths in the Ti_8C_{12} molecule differ by nearly a factor of 1.5 and equal $3.76a_0$ and $2.63a_0$ ($a_0 = 0.052918$ nm is the radius of the first Bohr orbit), respectively. According to Reddy *et al.*,[36] the Ti–C bond is ~30% longer than the C–C bond. On the other hand, the distances from carbon and titanium atoms to the centre of the cluster are nearly equal. This means that the real dodecahedral structure of Ti_8C_{12} is strongly distorted. The bonding states of the cluster Ti_8C_{12} are thought to be composed of the Ti *d*-AOs and the C_2 MOs while the Fermi level lies between the bonding and antibonding states of titanium, thus providing stability for the cluster.[35] Analogous conclusions that clusters M_8C_{12} have a distorted rather than ideal pentagondodecahedron shape were obtained in calculations reported by other authors.

Comparative analysis of the electronic structure of the Ti_8C_{12} met-car of T_h and T_d† symmetry showed [37] that in both structural types the highest occupied energy level corresponds to a sharp peak of the density of states (DOS) composed mainly of the C2*p*- and Ti3*d*-AOs. High chemical stability of compound Ti_8C_{12} is due to a combination of strong Ti3*d*–C2*p* interactions between the titanium atoms and C_2 unit on the one hand and to the C–C interactions in the carbon units on the other hand. In both structural types, Ti_8C_{12} has an open electron shell and can therefore be both electron acceptor and donor.

The atoms in met-car molecules are tightly bound. For instance, the bond energy in the Ti_8C_{12} molecule is 6.1–6.7 eV per atom.[35,36,38] For comparison, this parameter is 7.4–7.6 eV per atom for C_{60} fullerene molecule (see Refs 109, 110) and 7.2 eV per atom for titanium carbide TiC with the *B*1 (NaCl)-type fcc structure.[35]

Modern concepts of the geometry and electronic structure of molecular clusters Ti_8C_{12} (see Refs 29, 35–38) provide good explanation for their chemical stability and specific features of the reactivity towards both polar and nonpolar compounds. Combination of high reactivity and stability of Ti_8C_{12} clusters was confirmed experimentally.[111]

Molecular cluster Ti_8C_{12} has been the most detailed studied new compound in the Ti–C system; however, no macroscopic amounts of this substance were obtained so far.

† Calculations for T_h and T_d symmetry were carried out using the structure parameters and interatomic distances reported by Reddy *et al.*[36] and by Lin and Hall,[29] respectively.

2. Polymorphous modification of dicarbide TiC_2

Comparative analysis of the electronic structure of hypothetical metastable polymorphous modifications of carbide $TiC_{1.0}$ with the *B*2 (CsCl)-, *B*8 (NiAs)-, *B*3- and *B*4 (sphalerite and würtzite ZnS)-type structures and that of the real carbide $TiC_{1.0}$ with the *B*1-type structure showed [112] that search for new stable modifications of titanium carbide should be performed among those substances that are structurally similar to or derived from the *B*1 type.

Titanium dicarbide, which can have several types of crystal structure, was studied as a representative of this group of substances.[112, 113] The ThC_2-type monoclinic structure (space group $C2/c$) has a tetrahedral body-centred metal sublattice while the C_2 units occupy the octahedral interstices. In the CaC_2 ($C11a$)-type tetragonal body-centred structure [space group $I4/m$ (C^5_{4h})] the C_2 units also occupy octahedral interstices. The $C11a$ structural type can be derived from the *B*1-type lattice by extending it along the *c* axis; sites in the non-metal sublattice are occupied by the C_2 units oriented along the *c* axis. The unit cell of titanium dicarbide with this structural type comprises two formula units TiC_2 (Fig. 12). The atomic coordinates in the unit cell are listed in Table 4; the running coordinate of carbon atoms, $z/c = 0.427$, was determined assuming the same length of all Ti–C distances in the unit cell because each type of atom occupies sites of the same type. Figure 13 presents the X-ray diffraction pattern of tetragonal TiC_2 calculated using the atomic coordinates listed in Table 4.

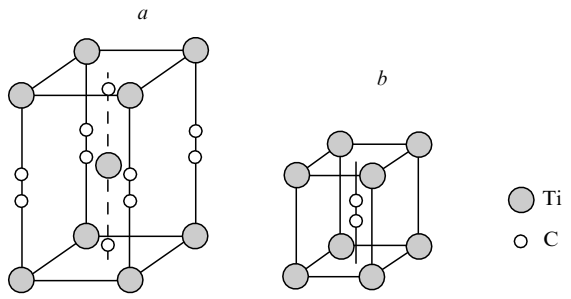


Figure 12. Unit cells of body-centred tetragonal TiC_2 with the CaC_2 ($C11a$)-type structure, space group $I4/m$ (C^5_{4h}) (*a*), and with the CsCl (*B*2)-type structure, space group $P4/mmm$ (D^1_{4h}) (*b*).

The non-metal sublattice of titanium dicarbide with the *B*2 (CsCl)-type tetragonal structure [space group $P4/mmm$ (D^1_{4h})] is built of C_2 units. The unit cell of this structure comprises one

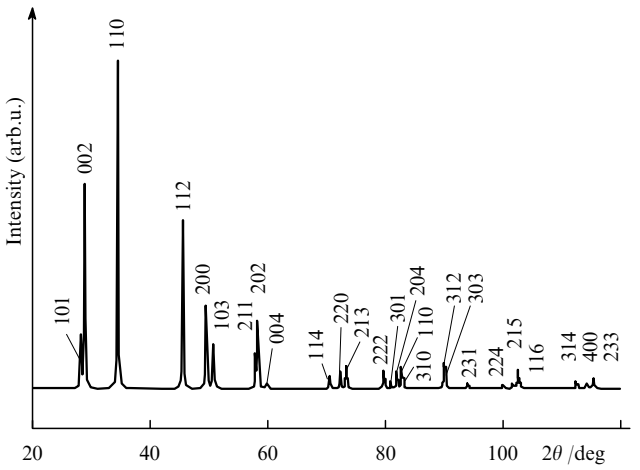


Figure 13. X-Ray diffraction pattern of tetragonal TiC_2 with the CaC_2 ($C11a$)-type structure, space group $I4/m$ (C^5_{4h}). Calculated for $CuK_{\alpha 1,2}$ radiation.

formula unit TiC_2 (see Fig. 12). The atomic coordinates in the unit cell are listed in Table 4. The running coordinate, z/c, of carbon atoms remains unknown so far and can vary between 0 and 0.5. The C–C separation in the C_2 unit is 0.124 nm; in titanium dicarbide this distance should be somewhat longer due to titanium–carbon interatomic interactions. This suggests that the most probable z/c values lie between 0.25 and 0.31. Figure 14 presents the X-ray diffraction patterns of tetragonal titanium dicarbide TiC_2 (space group $P4/mmm$) calculated for several different positions of the carbon atom ($z = 0.10$, 0.25, 0.30 and 0.40). Position of the carbon atom has a strong effect on the intensity ratio of diffraction reflections, namely, an increase in *z* from 0.1 to 0.4 causes a decrease in the intensities of the (001) and (111) reflections and an increase in the intensity of the (101) reflection.

Similarly to cubic monocarbide TiC_y, in titanium dicarbide with the CaF_2 ($C1$)-type cubic structure [space group $Fm\bar{3}m$ (O^5_h)] (Fig. 15) titanium atoms form a face-centred metal sublattice. However, carbon atoms occupy tetrahedral rather than octahedral (as in TiC_y) interstices. Naturally, the lattice constant of titanium dicarbide must be larger than that of titanium monocarbide, since only in this case is the size of the tetrahedral interstice sufficient to contain a carbon atom. Analysis of the crystal structure of cubic TiC_2 showed that it is a typical representative of interstitial phases. In the nondistorted crystal

Table 4. Crystal-chemical characteristics of possible (model) modifications of titanium dicarbides.

Dicarbide structure	Space group	Unit cell parameters /nm			Atomic coordinates in the unit cell					
		a	*b*	*c*	atom	position	*x*/*a*	*y*/*a*	*z*/*a*	*z*/*c*
Tetragonal CaC_2 ($C11a$)	$I4/m$ (C^5_{4h})	0.3668	–	0.617	Ti	2 (*a*)	0	0	–	0
					C	4 (*e*)	0	0	–	0.427
Tetragonal (derived from CsCl-type structure)	$P4/mmm$ (D^1_{4h})	0.2594	–	0.337	Ti	1 (*a*)	0	0	–	0
					C	2 (*h*)	1/2	1/2	–	–
Cubic of the CaF_2 type ($C1$)	$Fm\bar{3}m$ (O^5_h)	0.487	–	–	Ti	4 (*a*)	0	0	0	–
					C	8 (*c*)	1/4	1/4	1/4	–
Monoclinic of the ThC_2 type (see[a])	$C2/c$ (C^6_{2h})	0.510	0.310	0.510	Ti	4 (*e*)	0	0.2	0.25	–
					C	8 (*f*)	0.30	0.13	0.05	–
Cubic	$F\bar{4}3m$ (T^2_d)	0.588	–	–	Ti	4 (*a*)	0	0	0	–
					C1	4 (*b*)	1/2	1/2	1/2	–
					C2	4 (*d*)	3/4	3/4	3/4	–

[a] The angle β in the unit cell is 103.9 °.

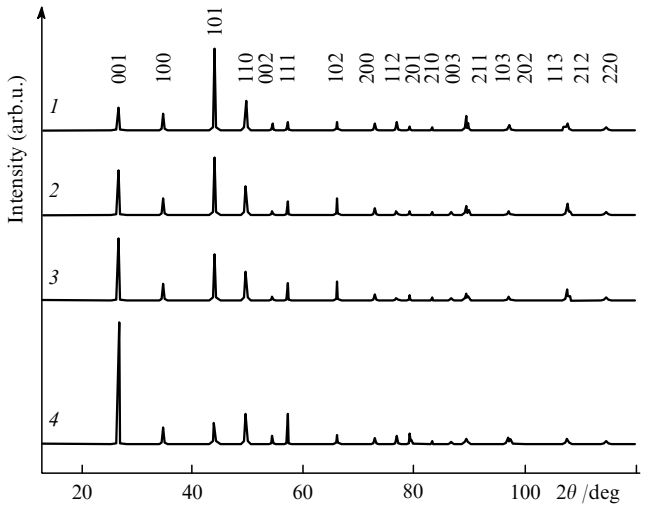


Figure 14. Effect of the position of carbon atom (z) in the unit cell of tetragonal TiC_2 with the CsCl-type structure (space group $P4/mmm$, $a = 0.2594$, $c = 0.337$ nm) on the intensity ratio of diffraction reflections (calculated for $CuK_{\alpha 1,2}$ radiation).
$z = 0.40$ (*1*); 0.30 (*2*); 0.25 (*3*) and 0.10 (*4*).

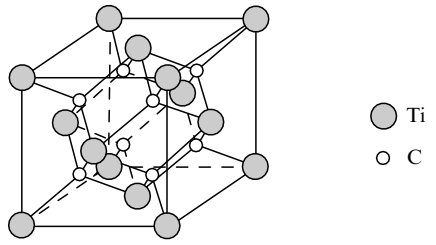


Figure 15. Unit cell of cubic TiC_2 with the CaF_2 ($C1$)-type structure, space group $Fm\bar{3}m$ (O_h^5).

lattice of this compound each carbon atom has a regular tetrahedral environment (four titanium atoms) while each titanium atom is surrounded by eight carbon atoms arranged at the cube vertices. The unit cell of cubic titanium dicarbide comprises four TiC_2 formula units. The calculated X-ray diffraction pattern of this dicarbide is shown in Fig. 16.

The electronic energy spectrum of hypothetical titanium dicarbide TiC_2 with the ThC_2-type monoclinic structure [space group $C2/c$ (C_{2h}^6)] was calculated.[112, 113] The lattice constants of this compound are $a = c = 0.510$ and $b = 0.310$ nm.[112] The unit

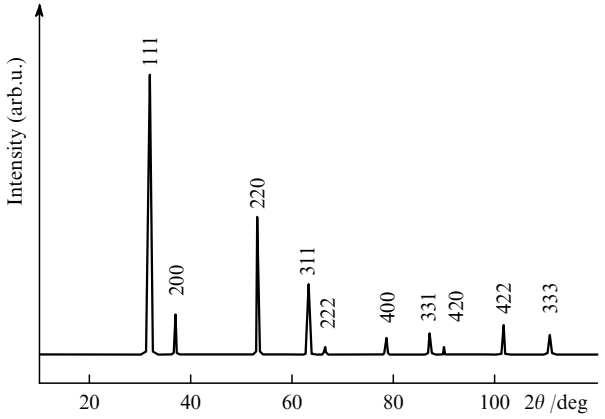


Figure 16. X-Ray diffraction pattern of cubic TiC_2 with the CaF_2 ($C1$)-type structure, space group $Fm\bar{3}m$ (O_h^5). Calculated for $CuK_{\alpha 1,2}$ radiation.

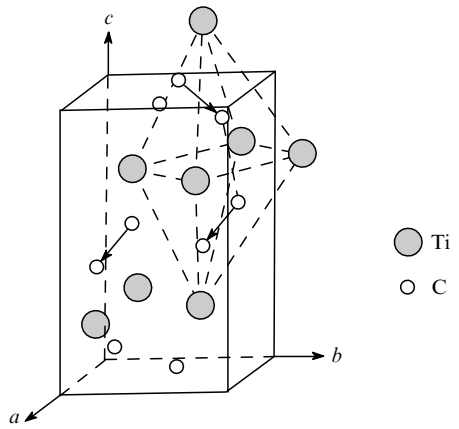


Figure 17. Unit cell of monoclinic TiC_2 with the ThC_2-type structure, space group $C2/c$ (C_{2h}^6). The two Ti atoms and one C atom arranged beyond the unit cell are also shown.

cell of monoclinic titanium dicarbide constructed using the atomic coordinates for monoclinic ThC_2 (see Ref. 114) is shown in Fig. 17 (the atomic coordinates in the unit cell are listed in Table 4). The unit cell comprises four formula units TiC_2. Distorted octahedra built of six titanium atoms contain two asymmetrically arranged carbon atoms (connected by a dashed line) separated by 0.251 nm. Atoms of the C_2 units are shared by two neighbouring octahedra while the C—C bonds pass through their common edges; the C—C distance in the C_2 units is 0.097 nm (in Fig. 17, the atoms of these units are shown connected by an arrow). The X-ray diffraction pattern calculated for polycrystalline dicarbide TiC_2 with this unit cell is shown in Fig. 18.

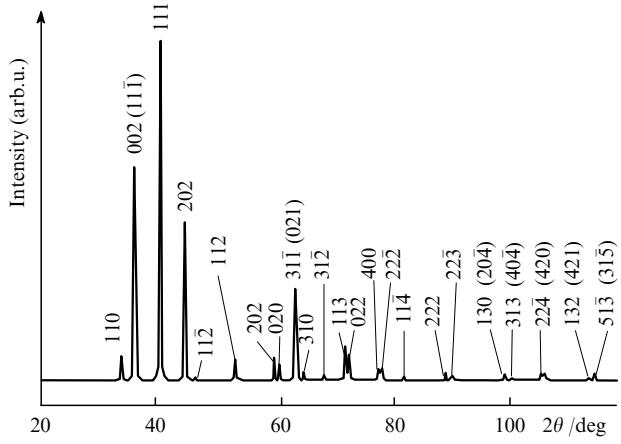


Figure 18. X-Ray diffraction pattern of monoclinic TiC_2 with the ThC_2-type structure, space group $C2/c$ (C_{2h}^6). Calculated for $CuK_{\alpha 1,2}$ radiation.

In polymorphous modifications of TiC_2 with the CaC_2-, CsCl-, CaF_2- and ThC_2-type structures the Fermi level lies in the region of delocalised d-states of titanium;[112, 113] therefore, all the four TiC_2 modifications behave as metals. The most stable is dicarbide with the ThC_2-type monoclinic structure. In dicarbide with the CaC_2-type structure the C—C bonds in C_2 units are the strongest, whereas the Ti—C bonds are poorly populated and, hence, weaker. Calculations for cubic TiC_2 with the CaF_2-type structure showed the absence of C—C bonds. According to calculations of the electronic structure of titanium dicarbides with the CaC_2- and ThC_2-type structures, the density of electron states at the Fermi level depends on the orientation of C_2 units in the crystal lattice. This implies the possibility of modifying the

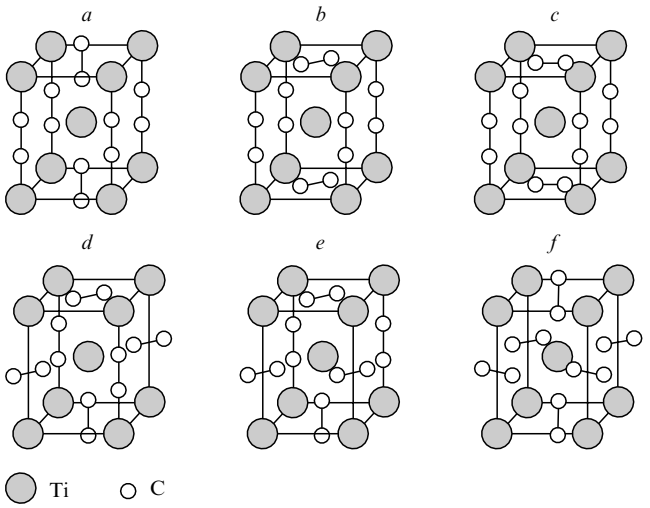


Figure 19. Arrangement of C_2 dimers in hypothetical titanium dicarbide with body-centred tetragonal structure of the CaC_2 (YC_2) type (*a*) and possible orientation disorder types of the carbon dimers (*b*–*f*).[112]

electronic structure and properties of titanium dicarbide by means of orientation ordering of the C_2 units.

Some of the possible types of orientation ordering of C_2 units are shown in Fig. 19.[112,113] The simplest form has the electronic spectrum of dicarbide TiC_2 with ordered CaC_2-type structure (see Fig. 19 *a*). Changes in the orientation of a fraction of C_2 units are accompanied by complication of the DOS distribution profile and by the appearance of new peaks. The most probable orientation type of C_2 units is to some extent similar to the ThC_2-type structure (Fig. 19 *d*).[112] The least probable is the orientation of a fraction of C_2 units along the edges of the unit cell (Fig. 19 *c*).

Experimental studies concerning the search for titanium dicarbide are scarce. A carbon–titanium compound with the concentration of bound carbon of greater than 50 at.% was first obtained in the high-temperature interaction of ethylene with titanium tetrachloride (gas-phase synthesis).[115] The carbide thus obtained had a CsCl-type cubic lattice with a lattice constant of 0.313 nm and was thought to have a TiC_2 composition. However, attempts at reproducing these results[115] failed.

A recent microdiffraction study[116] on films prepared by ion sputtering of carbon and titanium followed by vapour deposition revealed the formation of a compound with a body-centred lattice and composition TiC_2. The deposition temperature was varied from 330 to 770 K; thin films were deposited on fresh KCl cleavages, coatings 10 to 18 μm thick were obtained on glassy substrates. Films condensed at 330 K and annealed at 700 K for 3 h contained only titanium monocarbide. As the deposition (condensation) temperature increased from 330 to 620 K, the phase composition of the films remained unchanged; however, the fcc lattice constant of titanium carbide in these films reached ~0.455 nm at a carbon content of greater than 65 at.%. A gas-phase electron diffraction study also revealed a decrease in the intensity of reflections accompanied by an increase in the diffuse background at a carbon content of greater than 60 at.%. The electron diffraction patterns of the films containing ~65 at.% of carbon and deposited at 670 K exhibited three diffuse lines assigned to the body-centred lattice with a lattice constant of ~0.3 nm. A homogeneous film was prepared by condensation at 770 K; the partial pressure of reactants (gaseous carbon and titanium) was 8×10^{-8} Pa, the film growth rate was ~0.1 nm s^{-1} and the content of carbon in the vapours was ~66 at.%. The results obtained allowed one to suggest the formation of TiC_2 films, a body-centred lattice of this compound with a lattice constant of 0.294 nm and the structure of titanium dicarbide.

The results reported by Perekrestov and Pavlov[116] and especially their interpretation provoke some objections. First of all, no direct determination of film composition was made (at best, the content of carbon in the gas flow was monitored indirectly). The proposed crystal lattice structure of TiC_2 is not body-centred. This is a cubic lattice [space group $F\bar{4}3m$ (T_d^2)] with a face-centred metal (titanium) sublattice and a diamond-like non-metal (carbon) sublattice [*A*4 type, *i.e.*, two face-centred lattices displaced by (1/4 1/4 1/4) with respect to each other]. In the unit cell of this structure (Fig. 20) half of the carbon atoms occupy the octahedral interstices of the titanium sublattice, while the rest of the carbon atoms occupy half of the tetrahedral interstices of the titanium sublattice, so each of them is tetrahedrally surrounded by four titanium atoms and by four carbon atoms. This unit cell comprises four formula units TiC_2 and the lattice constant is 0.588 nm. The atomic coordinates in the cubic unit cell of TiC_2 (space group $F\bar{4}3m$) are listed in Table 4 and the calculated X-ray diffraction pattern is presented in Fig. 21.

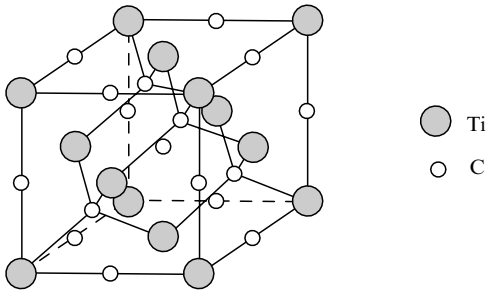


Figure 20. Unit cell of cubic TiC_2, space group $F\bar{4}3m$ (T_d^2), a = 0.588 nm.

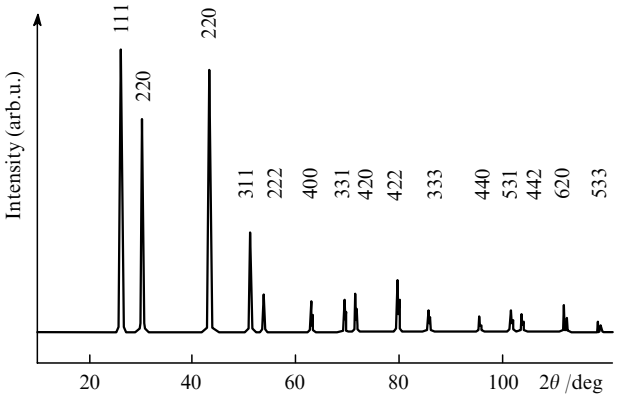


Figure 21. X-Ray diffraction pattern of polycrystalline cubic TiC_2, space group $F\bar{4}3m$ (T_d^2), a = 0.588 nm. Calculated for Cu$K_{\alpha 1,2}$ radiation.

In addition to clusters M_8C_{12} (see Section III.1), laser-assisted plasmachemical synthesis led to the formation of cluster-type nanoparticles M_mC_n (M = Ti, Zr, Hf, V; $m:n \approx 1:2$).[28,30,31] For M = Ti, molecular clusters of composition $Ti_{13}C_{22}$ were usually formed (*i.e.*, the titanium : carbon ratio was close to the corresponding parameter in ideal TiC_2). Preferable formation of nanoclusters with a high content of carbon (M : C ≈ 1 : 2) occurred at a high concentration of hydrocarbon in the gas phase and at an increased laser power, which led to an increase in the hydrogenation degree of the hydrocarbon and, correspondingly, to an increase in the content of carbon in the plasma.

Thus, analysis of the available data suggests that titanium dicarbide TiC_2 can belong to five structural types. These are the ThC_2-type monoclinic structure [space group $C2/c$ (C_{2h}^6)]; CaC_2 ($C11a$)- and CsCl ($B2$)-type tetragonal structures with $I4/m$ (C_{4h}^5) and $P4/mmm$ (D_{4h}^1) space groups, respectively; CaF_2 ($C1$)-type cubic structure [space group $Fm\bar{3}m$ (O_h^5)] and a cubic structure

with a diamond-like carbon sublattice and the $F\bar{4}3m$ (T_d^2) space group.

3. Endohedral fullerene Ti@C_{28} and rhombohedral titanium carbide

The discovery of C_n fullerenes ($n = 60-90$) (see Refs 70–73, 117, 118) and further studies of these compounds showed that the C_n clusters containing less than 60 carbon atoms are of low stability. Fullerenes with a small number of atoms (*e.g.*, C_{28} fullerene) can be stabilised by preparing endohedral complexes M@C_{28} in which the dopant atom is placed inside the carbon sphere. A Ti@C_{28} endohedral complex was also synthesised.[119]

The possibility of stabilising unstable C_{28} fullerene by intercalating it with both non-metal atoms of 2*p*-elements (B, C, N and O) and metals (3*d*-elements such as Sc, Ti, V, Cr, Fe and Cu) was studied theoretically.[112, 120] When estimating the formation probability of endohedral M@C_{28} complexes with 3*d*-metals, one can take into account the geometric, chemical and kinetic factors. In the case of C_{28} fullerene the maximum radius of a metal ion that can be placed inside the carbon sphere lies between 0.09 and 0.10 nm (see Ref. 121); all 3*d*-metals fulfil this geometric criterion. The chemical factor is favourable if electron density transfer as a result of intercalation favours an increase in the bonding character of the MOs. The kinetic factor includes the formation mechanism of endohedral complexes. They are prepared by rolling a graphene sheet around the metal atom adsorbed on the graphite surface. This can occur if the interaction between the metal and the graphite surface causes strengthening of the M–C bonds and weakening of the C–C bonds (especially of the interlayer bonds). Recent studies [112, 120] showed that intercalation of metal atoms is accompanied by electron density transfer from these atoms to the atoms of the fullerene cage, by changes in the populations of the overlapping C-AOs, by the formation of the M–C bond and by a change in the pattern of the electronic energy spectrum.

The endohedral complex Ti@C_{28} with the Ti atom at the centre of the C_{28} polyhedron was shown to be the most stable (with inclusion of the chemical and kinetic factors).[120] Probably, this complex can be considered as a possible molecular cluster-like compound that can be formed in the Ti–C system.

The results of a recent study [122] on the electronic structure of hypothetical metastable polymorphous modifications of $TiC_{1.0}$ prompted us to mention a study by Dubrovinskaia *et al.*[122] who experimentally found a rhombohedral modification of titanium carbide. The sample of cubic titanium carbide (no composition was reported) with a lattice constant of 0.4327 nm was subjected to quasi-hydrostatic pressure ($\sim$10 GPa) at 300 K. This resulted in broadening of the diffraction reflections of the *B*1-type cubic structure and in splitting of the $(111)_{B1}$ reflection into two lines corresponding to the rhombohedral structure at a pressure of 18 and 38 GPa. The authors believed that rhombohedral distortion of the cubic unit cell is due to extension of its [111] diagonal, which led to splitting of the $(111)_{B1}$ reflection into the (003) and (101) rhombohedral lines and to splitting of the $(200)_{B1}$ reflection into the (104) and (110) lines. Rhombohedral titanium carbide prepared at a pressure of 38 GPa has a unit cell with the lattice constants $a = 0.29442$ and $c = 0.73354$ nm (in a hexagonal setting).

IV. Ordered phases of nonstoichiometric titanium carbide TiC_y

The ordering of interstitial atoms was experimentally found for most of the nonstoichiometric transition metal carbides, nitrides and oxides. In disordered nonstoichiometric compounds the interstitial atoms and structural vacancies form a substitution solution in the non-metal sublattice, all sites of the non-metal sublattice being crystallographically equivalent. Ordering causes redistribution of the interstitial atoms and vacancies over sites of the non-metal sublattice, thus making the lattice sites inequivalent. The crystal lattice is divided into at least two sublattices differing in site occupation probabilities by the atoms of the same sort. Ordering is accompanied by symmetry reduction of the crystal, since some of the symmetry elements of a disordered non-metal sublattice that match the occupied and vacant sites do not belong to the group of symmetry elements of the ordered crystal in which these sites become crystallographically inequivalent.

From the aforesaid it follows that the nonstoichiometry responsible for the fact that the number of interstitial sites is larger than that of atoms occupying these sites is a prerequisite to the ordering in defect carbides.

Description of different ordered phases of nonstoichiometric carbides, nitrides, oxides and their solid solutions can be found in reviews [1, 22, 123–127] and monographs.[2, 3, 14, 17, 27, 70]

Compared to other carbides (except for vanadium carbide VC_y), the ordering in nonstoichiometric titanium carbide TiC_y with the *B*1-type cubic structure has been studied in most detail; however, the mechanism of this process is still to be clarified. A great body of experimental information on the chemical composition and structure of ordered phases of titanium carbide TiC_y published earlier has not been confirmed later. The main characteristics of both experimentally observed and theoretically calculated ordered phases of nonstoichiometric titanium carbide are listed in Table 5.

As mentioned above, disordered titanium carbide TiC_y ($TiC_y\square_{1-y}$) is characterised by an extremely broad homogeneity region from $TiC_{0.48}$ to $TiC_{1.00}$ (see Refs 2, 3, 14). Within this region, carbon atoms and structural vacancies $\square$ form a substitution solution in the non-metal sublattice. Depending on the composition and the synthesis and heat treatment conditions, TiC_y can exist in a disordered or ordered state. The disordered state is in thermodynamic equilibrium at $T > 1100$ K, while the ordered state is in thermodynamic equilibrium at $T < 1000$ K. Due to the low diffusive mobility of the atoms, the disordered state of nonstoichiometric titanium carbide is retained upon quenching from $T > 1100$ K to rather low temperatures ($\sim$300 K) and exists as a metastable state at $T < 1000$ K.

Order-parameter functional (OPF) calculations[1–3, 18, 20, 22] showed that monocarbide TiC_y can form three ordered phases of compositions Ti_2C, Ti_3C_2 and Ti_6C_5. According to the inverse Monte Carlo calculations performed for a narrower composition range from $TiC_{0.55}$ to $TiC_{0.70}$ (see Ref. 12), the ordered phases Ti_2C and Ti_3C_2 are in thermodynamic equilibrium at $T < 950$ K, which is in agreement with the results of the above-mentioned calculations.[1–3, 18, 20, 22] Experimental studies of carbide TiC_y in the composition range $0.5 \leqslant y < 0.7$ revealed the existence of ordered phases of the Ti_2C type with cubic (space group $Fd\bar{3}m$) and trigonal (space group $R\bar{3}m$ or $P3_121$, the former being more probable) symmetry (see Table 5), orthorhombic ordered phase Ti_3C_2 (space group $C222_1$) and hexagonal ordered phase Ti_6C_5 (see Ref. 130). The trigonal ordered phase Ti_8C_5 (space group $R\bar{3}m$) was reported erroneously. Virtually no studies of the ordering of TiC_y ($y > 0.7$) were performed until the mid-1990s.

Let us consider in more detail which ordered phases of the compositions Ti_2C and Ti_3C_2 can be formed in nonstoichiometric carbide TiC_y.

According to different studies of TiC_y, an ordered phase of composition Ti_2C with cubic (space group $Fd\bar{3}m$) (see Refs 9, 46–48, 50) or trigonal (space group $R\bar{3}m$) (see Refs 12, 49) symmetry is formed in the range $0.5 \leqslant y \leqslant 0.65$ at $T < 1100$ K.‡ Cubic Ti_2C phase is thought to be metastable. Initially,[49, 129] the cubic phase was assumed to have a higher T_{trans}

‡ Information on the existence of the trigonal (space group $P3_121$) Ti_2C (Ti_6C_{3+x}) phase is erroneous: formation of a trigonal (space group $P3_121$) M_2C-type phase with the unit cell parameters $a = b = a_{B1}/\sqrt{2}$ (**a** = {1/2 1/2 0}$_{B1}$) and $c = 3\sqrt{2} \times a_{B1}$ (**c** = {222}$_{B1}$) based on the basic *B*1-type structure is impossible, since in this case the sites of the metal and non-metal sublattices partially match one another.

Table 5. Characteristics of ordered phases of nonstoichiometric titanium carbide TiC_y with cubic *B*1-type structure.

Composition	Existence region	Symmetry (lattice type)	Space group	Unit cell parameters /nm	Ref.	Note [a]
Ti_2C	$TiC_{0.52}$–$TiC_{0.71}$	cubic	$Fd\bar{3}m$	$a = 2a_0$	9, 48	carbon sublattice is partially ordered; $T_{trans} \approx 950$–1030 K
Ti_2C	$TiC_{0.58}$–$TiC_{0.63}$	trigonal	$R\bar{3}m$	$a = b = c = (a_0\sqrt{6})/2$	12, 128	calculated; $T_{trans} < 900$ K; the homogeneity region corresponds to 750 K
Ti_3C_2	$TiC_{0.64}$–$TiC_{0.68}$	orthorhombic	$C222_1$	$a = a_0\sqrt{2}$, $b = 3a_0\sqrt{2}$, $c = 2a_0$	12, 129	calculated; $T_{trans} < 720$ K; the homogeneity region corresponds to 650 K
Ti_2C	$TiC_{0.49}$–$TiC_{0.54}$	cubic	$Fd\bar{3}m$	$a = 2a_0$	21	$T_{trans} < 1000$ K; the homogeneity region corresponds to ~600 K
Ti_2C	$TiC_{0.55}$–$TiC_{0.59}$	trigonal	$R\bar{3}m$	$a = b = c = (a_0\sqrt{6})/2$	21	$T_{trans} < 1010$ K; the homogeneity region corresponds to ~600 K
Ti_3C_2	$TiC_{0.63}$–$TiC_{0.67}$	orthorhombic	$C222_1$	$a = a_0\sqrt{2}$, $b = 3a_0\sqrt{2}$, $c = 2a_0$	21	$T_{trans} < 990$ K; the homogeneity region corresponds to ~600 K
Ti_6C_5	–	hexagonal	–	$a = b = (a_0\sqrt{6})/2 = 0.529$, $c = (4a_0\sqrt{3})/3 = 0.996$	130	phase was found in thin films
Ti_2C	$TiC_{0.47}$–$TiC_{0.54}$	–	–	–	18, 20, 22	calculated; $T_{trans} < 950$ K; the homogeneity region corresponds to 600 K
Ti_3C_2	$TiC_{0.62}$–$TiC_{0.70}$	–	–	–	18, 20, 22	calculated; $T_{trans} < 930$ K; the homogeneity region corresponds to 600 K
Ti_6C_5	$TiC_{0.80}$–$TiC_{0.90}$	–	–	–	18, 20, 22	calculated; $T_{trans} < 920$ K; the homogeneity region corresponds to 600 K

[a] T_{trans} is the disorder–order transformation temperature.

value than the trigonal phase, thus being an intermediate ordered high-temperature phase with respect to the disordered phase and low-temperature trigonal phase of composition Ti_2C. Tashmetov *et al.*[131] reported a consecutive phase transformation

$$\text{disordered phase (space group } Fm\bar{3}m) \overset{1070\text{ K}}{\rightleftharpoons} \rightleftharpoons \text{ cubic ordered phase (space group } Fd\bar{3}m) \overset{1050\text{ K}}{\rightleftharpoons} \rightleftharpoons \text{ trigonal ordered phase (space group } R\bar{3}m).$$

However, de Novion *et al.*[12] suggested that in TiC_y ($y \geqslant 0.58$) the cubic phase Ti_2C can exist as a metastable phase for which T_{trans} is ~10 K lower than for the trigonal ordered phase.

Analysis of the results of experimental structural studies [9, 12, 46–50, 128, 131] showed that cubic superstructure Ti_2C is usually found in annealed TiC_y samples with $y < 0.55$–0.56, whereas the samples with $0.58 \leqslant y \leqslant 0.65$ are characterised by trigonal ordering. It should be noted that the X-ray diffraction patterns of both cubic and trigonal ordered phases of composition Ti_2C exhibit identical sets of superstructure reflections and can be distinguished only given trigonal distortions in the phase with the space group $R\bar{3}m$ and taking into account the directions of static atomic displacements.[126] Probably, this is the reason for attributing the observed superstructure reflections in annealed carbide TiC_y ($y \geqslant 0.59$) to the cubic phase Ti_2C in the studies [46–48, 50] concerned with the cubic model of ordering.[9] Other authors [12, 49, 128, 129, 131] showed that trigonal phase Ti_2C is the major ordered phase of TiC_y ($y \geqslant 0.6$).

The assumption of the existence of ordered phase Ti_3C_2 in the composition range $TiC_{0.60}$–$TiC_{0.70}$ was confirmed by some experimental studies. An elastic neutron scattering study [129] of annealed single crystal $TiC_{0.61}$ revealed the presence of the (2/3 2/3 0) superstructure reflections. The X-ray diffraction pattern of annealed carbide $TiC_{0.70}$ exhibited weak superstructure reflections with the reduced diffraction vector $|\mathbf{q}| \approx 2.03$ characteristic of the orthorhombic phase Ti_3C_2 (space group $C222_1$).[132] Diffuse neutron scattering maxima corresponding to the (2/3 2/3 0) reflections and due to short-range order in $TiC_{0.76}$ were detected.[133] Estimation of the short-range order parameters in a single crystal of composition $TiC_{0.64}$ [12] using the diffuse neutron scattering data showed that agreement between the calculated and experimental data is the best when annealed carbide $TiC_{0.64}$ contained a mixture of two ordered phases Ti_2C and Ti_3C_2. The existence of a trigonal phase Ti_3C_2 was also confirmed by the OPF [18, 20, 22] and Monte Carlo [10, 12] calculations. A theoretical study[18] also suggested the formation of an ordered phase Ti_6C_5 in carbide TiC_y ($0.78 < y < 0.88$). The calculated disorder–order transformation temperatures for the Ti_3C_2 and Ti_6C_5 phases did not exceed 950 K.[18, 20, 22]

The structure of the ordered phases of nonstoichiometric carbide TiC_y has been studied in detail.[21]

Samples of nonstoichiometric titanium carbide TiC_y with different carbon content ($0.52 \leqslant y \leqslant 0.98$) were synthesised by hot pressing the mixtures of $TiC_{0.98}$ and metallic titanium powders ($T = 1773$–2173 K, $p = 20$–30 MPa) in highly pure argon atmosphere for 30 min or by solid-phase vacuum sintering the $TiC_{0.94}$, carbon black and metallic titanium powders ($T = 2000$ K, $p = 0.001$ Pa) for 6 h. The ordered state of the carbides obtained was achieved by annealing the samples with gradual lowering of the temperature from 1070 down to 770 K for 340 h. Annealing resulted in the appearance of superstructure reflections in the X-ray diffraction patterns of carbides $TiC_{0.50}$, $TiC_{0.52}$, $TiC_{0.54}$, $TiC_{0.55}$, $TiC_{0.58}$ and $TiC_{0.62}$.

The X-ray diffraction patterns of the annealed carbides $TiC_{0.50}$, $TiC_{0.52}$ and $TiC_{0.54}$ exhibited identical sets of superstructure reflections. The first superstructure reflection with the reduced wave vector $|\mathbf{q}| = (2a_{B1}\sin\theta)/\lambda \approx 0.870$ in the region $2\theta \approx 17.8$–17.9° corresponds to the vector {1/2 1/2 1/2} of length $|\mathbf{q}| \approx 0.866$. The next three superstructure reflections at $2\theta \approx 34.5$, 45.9 and 55.4° correspond to the vectors {3/2 1/2 1/2}, {3/2 3/2 1/2} and {3/2 3/2 3/2}. The {3/2 3/2 1/2} superstructure reflection is very weak. Taking into account the positions of the observed superstructure reflections and the absence of trigonal splitting of the $(331)_{B1}$, $(420)_{B1}$ and $(422)_{B1}$ lines, one can suggest that annealing led to the formation of the ordered cubic phase Ti_2C (space group $Fd\bar{3}m$) in carbides $TiC_{0.50}$, $TiC_{0.52}$ and $TiC_{0.54}$. The channel of disorder–order structural phase transformation TiC_y (space group $Fm\bar{3}m$) $\rightleftharpoons$ Ti_2C (space group

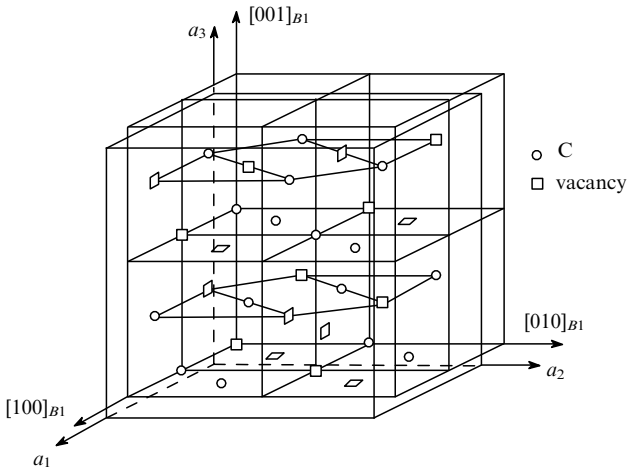


Figure 22. Cubic unit cell (space group $Fd\bar{3}m$) of the Ti_2C superstructure in the lattice with the $B1$-type structure (Ti atoms are not shown).[17, 27, 126]

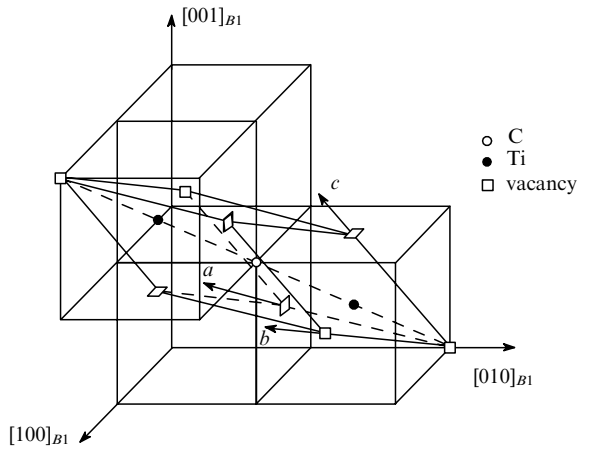


Figure 23. Trigonal unit cell (space group $R\bar{3}m$) of the Ti_2C superstructure in the lattice with the $B1$-type structure.[17, 27, 126]

$Fd\bar{3}m$) includes all four arms of the $\{\mathbf{k}_9\}$ Lifshitz star: $\mathbf{k}_9^{(1)} = (\mathbf{b}_1 + \mathbf{b}_2 + \mathbf{b}_3)/2, \mathbf{k}_9^{(2)} = \mathbf{b}_1/2, \mathbf{k}_9^{(3)} = \mathbf{b}_2/2$ and $\mathbf{k}_9^{(4)} = \mathbf{b}_3/2$.§

The unit cell of cubic superstructure M_2C (space group $Fd\bar{3}m$) is shown in Fig. 22. The translation vectors of and the atomic and vacancy coordinates in the unit cell are listed in Table 6. In completely ordered, ideal cubic superstructure M_2C all metal atoms occupy sites of the M_3^4 type (the subscript and superscript denote the number of vacancies in the first and second coordination sphere of the metal atom, respectively). The non-metal sublattice of this superstructure is characterised by alternation of the $(111)_{B1}$ atomic planes in which 1/3 and 2/3 of the total number of sites are vacant.

Table 6. Characteristics of cubic [space group $Fd\bar{3}m$ (O_h^7)] M_2C superstructure: $\mathbf{a}_1 = \langle 200\rangle_{B1}, \mathbf{a}_2 = \langle 020\rangle_{B1}, \mathbf{a}_3 = \langle 002\rangle_{B1}$.[16, 27, 126]

Atom	Position	Atomic coordinates in ideal ordered structure		
		x/a_1	y/a_2	z/a_3
C1 (vacancy)	16 (*c*)	1/8	1/8	1/8
C2	16 (*d*)	5/8	5/8	5/8
M1	32 (*e*)	3/8	3/8	3/8

The X-ray diffraction pattern of annealed carbide $TiC_{0.58}$ exhibited the {1/2 1/2 1/2}, {3/2 1/2 1/2} and {3/2 3/2 3/2} superstructure reflections at $2\theta \approx 17.9^\circ$, 34.4° and 55.4° (see Ref. 21). No {3/2 3/2 1/2} reflection was observed. An important distinction of the X-ray diffraction pattern of annealed carbide $TiC_{0.58}$ from those of annealed carbides of compositions $TiC_{0.50}$, $TiC_{0.52}$ and $TiC_{0.54}$ is the presence of trigonal splitting of the $(220)_{B1}$, $(311)_{B1}$, $(222)_{B1}$, $(331)_{B1}$, $(420)_{B1}$ and $(422)_{B1}$ lines. This is an indication of the trigonal ordered phase Ti_2C (space group $R\bar{3}m$) formed in carbide $TiC_{0.58}$ upon annealing.

The unit cell of the trigonal phase is shown in Fig. 23. Its translation vectors and the atomic and vacancy coordinates in ideal trigonal structure M_2C are listed in Table 7. The TiC_y (space group $Fm\bar{3}m$) $\rightleftharpoons$ Ti_2C (space group $R\bar{3}m$) disorder – order phase transition channel involving the formation of this superstructure includes one arm, $\mathbf{k}_9^{(3)} = \mathbf{b}_2/2$, of the $\{\mathbf{k}_9\}$ Lifshitz star.

§ For a detailed description of all stars $\{\mathbf{k}_s\}$ of the wave vectors of the first Brillouin zone and their arms for a crystal with a fcc lattice, see Refs 2, 3 and 70.

Table 7. Characteristics of trigonal space group [$R\bar{3}m$ (D_{3d}^5)] M_2C superstructure: $\mathbf{a}_{tr} = \frac{1}{2}\langle 1\bar{2}1\rangle_{B1}, \mathbf{b}_{tr} = \frac{1}{2}\langle 2\bar{1}1\rangle_{B1}, \mathbf{c}_{tr} = \frac{1}{2}\langle 1\bar{1}2\rangle_{B1}$.[16, 27, 126]

Atom	Position	Atomic coordinates in ideal ordered structure		
		x/a_{tr}	y/b_{tr}	z/c_{tr}
C1 (vacancy)	1 (*a*)	0	0	0
C2	1 (*b*)	1/2	1/2	1/2
M1	2 (*c*)	1/4	1/4	1/4

The non-metal sublattice of completely ordered trigonal structure M_2C (space group $R\bar{3}m$) is characterised by alternation of the $(1\bar{1}1)_{B1}$ atomic planes with completely occupied (by interstitial atoms) and completely vacant sites along the $[1\bar{1}1]_{B1}$ direction. This superstructure must have a highly distorted metal sublattice. In completely ordered, ideal trigonal superstructure M_2C all metal atoms occupy identical sites of the M_3^4 type with three vacancies in the first and four vacancies in the second coordination sphere.

The X-ray diffraction pattern of annealed carbide $TiC_{0.62}$ exhibited both the {1/2 1/2 1/2} ($2\theta \approx 18.0^\circ$) and {3/2 3/2 3/2} ($2\theta \approx 55.2^\circ$) superstructure reflections from the trigonal ordered phase Ti_2C (space group $R\bar{3}m$) and some other superstructure reflections that were absent in the X-ray diffraction patterns of the carbides of compositions $TiC_{0.50}$, $TiC_{0.52}$, $TiC_{0.54}$, $TiC_{0.55}$ and $TiC_{0.58}$ (see Ref. 21). These are the reflections in the ranges $2\theta \approx 30.6 - 30.7^\circ$, 41.2°, 42.6° and $55.4 - 55.5^\circ$ with reduced wave vectors of lengths $|\mathbf{q}| \approx 1.488$, 1.970, 2.038 and 2.607, respectively. The first two reflections are associated with the $\mathbf{k}_4^{(1)} = \{2/3\ 2/3\ 0\}$ and $\mathbf{k}_4^{(2)} = -\mathbf{k}_4^{(1)}$ arms of the $\{\mathbf{k}_4\}$ star, while the other two reflections are associated with the $\mathbf{k}_3^{(3)} = \{1/3\ -2/3\ -1/2\}$, $\mathbf{k}_3^{(4)} = -\mathbf{k}_3^{(3)}$, $\mathbf{k}_3^{(5)} = \{-1/3\ 2/3\ -1/2\}$ and $\mathbf{k}_3^{(6)} = -\mathbf{k}_3^{(5)}$ arms of the $\{\mathbf{k}_3\}$ star. This set of superstructure reflections can correspond only to the orthorhombic ordered phase Ti_3C_2 (space group $C222_1$). The transition channel involving the formation of this phase includes two arms of the $\{\mathbf{k}_4\}$ star and four arms of the $\{\mathbf{k}_3\}$ star (see Ref. 126). Characteristic of this superstructure are the $\{1/3\ -2/3\ -1/2\}$ and {2/3 2/3 0} reflections which should be observed in the regions $2\theta \approx 18.4^\circ$ and 19.4°, respectively. The experimental X-ray diffraction pattern in this interval of angles exhibited a slightly 'swollen' slope of the {1/2 1/2 1/2} superstructure reflection of the trigonal phase Ti_2C.[21]

The orthorhombic unit cell of the M_3C_2 superstructure is shown in Fig. 24. Its translation vectors and the atomic and

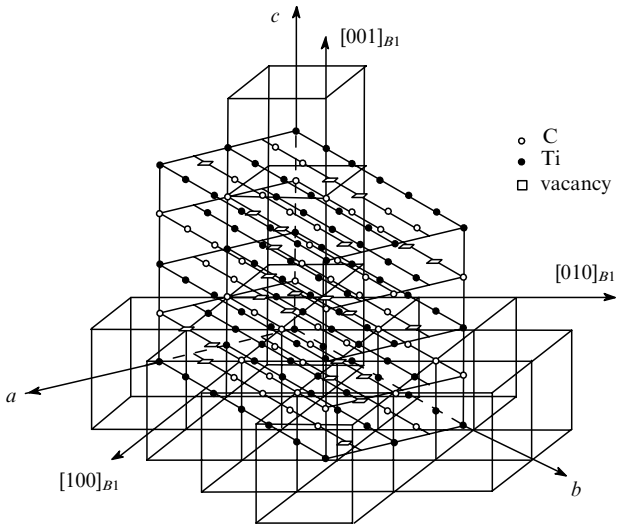


Figure 24. Orthorhombic unit cell (space group $C222_1$) of the Ti_3C_2 superstructure in the lattice with the $B1$-type structure.[2, 3, 17, 27, 126]

vacancy coordinates in this superstructure are listed in Table 8. The existence of orthorhombic ordered phase M_3C_2 (space group $C222_1$) of titanium carbide $TiC_{0.64}$ was suggested[12] based on the results of Monte Carlo simulations. In completely ordered orthorhombic structure M_3C_2 two thirds of all metal atoms occupy the sites of the type M_2^3 while the rest metal atoms occupy the sites of the type M_2^2.

Metallographic tests of annealed carbides $TiC_{0.50}$ and $TiC_{0.55}$ in reflected polarised white light showed that the former exhibited neither grain interference from the disordered phase nor surface precipitate interference from the ordered phase.[21] This can occur if both phases belong to the cubic crystal system. Particular grains of annealed carbide $TiC_{0.55}$ were coated with plate-like and prismatic precipitates of the ordered phase. The symmetry of these precipitates was different from that of the disordered phase while their shape was typical of the crystals that belong to the trigonal crystal system and, unlike the crystals of the disordered cubic phase, exhibit an interference pattern (*i.e.*, are anisotropic). Therefore, the results of diffraction studies of the ordered phases of non-stoichiometric carbide TiC_y were confirmed by the results of metallographic tests.

Thus, low-temperature annealing of carbide TiC_y leads to the formation of some ordered phases. These are the cubic phase Ti_2C (space group $Fd\bar{3}m$) in the composition range $TiC_{0.50}-TiC_{0.54}$, the trigonal phase Ti_2C (space group $R\bar{3}m$) for $TiC_{0.55}-TiC_{0.58}$ and the orthorhombic phase Ti_3C_2 (space group $C222_1$) in the range $TiC_{0.63}-TiC_{0.68}$.

Figure 25 presents the calculated X-ray diffraction patterns of the cubic and trigonal ordered phases Ti_2C formed in carbides of composition $TiC_{0.50}$ ($a_{B1} = 0.4305$ nm) and $TiC_{0.55}$ ($a_{B1} = 0.4310$ nm), respectively. The X-ray diffraction patterns were calculated assuming the maximum degree of long-range order characterised by the parameter η equal to 1.00 and 0.90 for the ordered carbides $TiC_{0.50}$ and $TiC_{0.55}$, respectively. The X-ray diffraction patterns of the cubic and trigonal ordered phases Ti_2C exhibit identical sets of superstructure reflections; however, distortion of the ideal lattice of the trigonal phase [slight extension along the $(1\ -1\ 1)_{B1}$ axis] leads to splitting of the $(311)_{B1}$, $(222)_{B1}$, $(420)_{B1}$ and $(422)_{B1}$ reflections. Trigonal splitting of the $(222)_{B1}$ reflection into two lines, *viz.*, the (0 0 12) and (0 2 4) lines, is shown in the inset in Fig. 25 *b* as an example; the doublet $\alpha_{1,2}$ is due to the use of $CuK_{\alpha 1,2}$ radiation. The superstructure reflections are of rather high intensity: for instance, the intensity of the first superstructure reflection is 30 times lower than that of the $(111)_{B1}$ reflection and only 3 times lower than the intensity of the $(222)_{B1}$ reflection. This makes the ordered phase Ti_2C readily detectable.

Table 8. Characteristics of orthorhombic [space group $C222_1$ (D_2^5)] M_3C_2 superstructure: $\mathbf{a}_{rh} = \langle 1\bar{1}0\rangle_{B1}$, $\mathbf{b}_{rh} = \langle 330\rangle_{B1}$, $\mathbf{c}_{rh} = \langle 002\rangle_{B1}$.[17, 27, 126]

Atom	Position	Atomic coordinates in ideal ordered structure		
		x/a_{rh}	y/b_{rh}	z/c_{rh}
C1 (vacancy)	4 (*b*)	0	1/6	1/4
C2 (vacancy)	4 (*b*)	0	1/3	1/4
C3 (vacancy)	8 (*c*)	1/4	5/12	0
C4	4 (*b*)	0	0	1/4
C5	4 (*b*)	0	1/2	1/4
C6	4 (*b*)	0	2/3	1/4
C7	4 (*b*)	0	5/6	1/4
C8	8 (*c*)	1/4	1/12	0
C9	8 (*c*)	1/4	1/4	0
M1	4 (*a*)	0	0	0
M2	4 (*a*)	1/2	0	0
M3	8 (*c*)	1/4	1/12	1/4
M4	8 (*c*)	1/4	1/4	1/4
M5	8 (*c*)	1/4	5/12	1/4
M6	8 (*c*)	0	1/6	1/2
M7	8 (*c*)	0	1/3	1/2

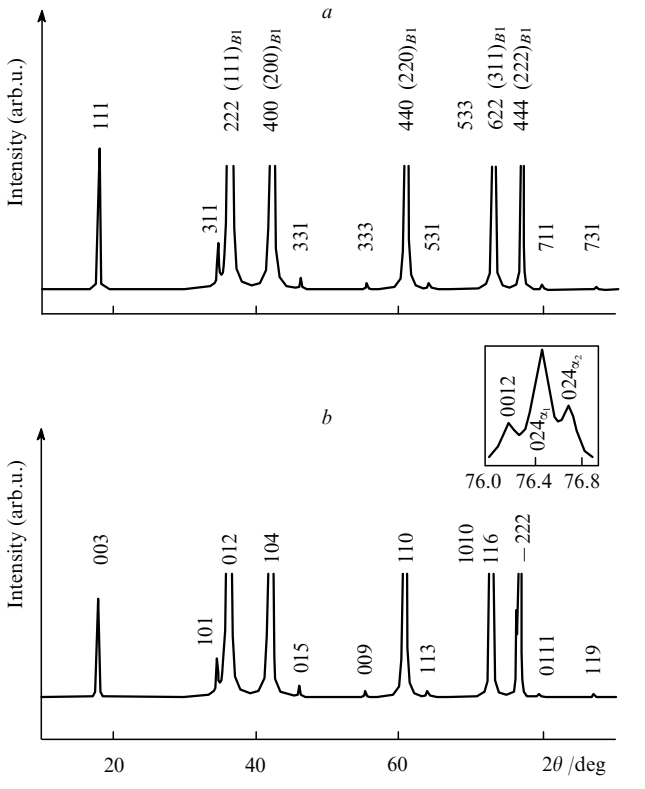


Figure 25. X-Ray diffraction patterns of cubic (space group $Fd\bar{3}m$, $a = 0.861$ nm) (*a*) and trigonal (space group $R\bar{3}m$, the lattice constants for hexagonal setting are $a = b = 0.3048$ and $c = 1.4982$ nm) (*b*) ordered Ti_2C phases formed in titanium carbide of the compositions $TiC_{0.50}$ ($a_{B1} = 0.4305$ nm) and $TiC_{0.55}$ ($a_{B1} = 0.4310$ nm), respectively. The long-range order parameter, $\eta = \eta_{max}$, equals 1 (*a*) and 0.90 (*b*).
The inset demonstrates trigonal splitting of the $(222)_{B1}$ reflection into the (0 0 12) and (0 2 4) lines due to slight extension of the basic cubic lattice along the $(1\ -1\ 1)_{B1}$ axis (lattice constant, $c = 1.4982$ nm, is increased compared to the value $c = 1.4930$ nm for the ideal trigonal cell). Calculated for $CuK_{\alpha 1,2}$ radiation.

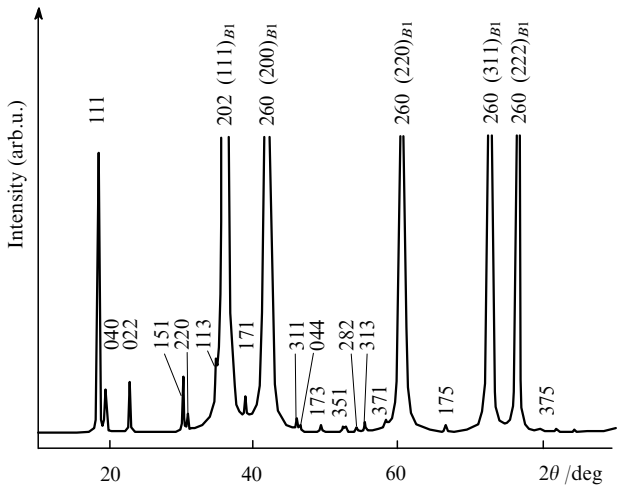


Figure 26. X-Ray diffraction pattern of the completely ordered ($\eta = 1.00$) orthorhombic Ti_3C_2 phase (space group $C222_1$, $a = 0.6109$, $b = 1.2328$ and $c = 0.864$ nm) formed in titanium carbide of composition $TiC_{0.667}$ ($a_{B1} = 0.432$ nm). Calculated for Cu$K_{\alpha 1,2}$ radiation.

The X-ray diffraction pattern of the ordered orthorhombic phase Ti_3C_2 (space group $C222_1$) formed in the carbide of composition $TiC_{0.667}$ is shown in Fig. 26. A characteristic feature of the orthorhombic superstructure Ti_3C_2 is the presence of three superstructure reflections in the range $19^\circ < 2\theta < 31^\circ$.

A hexagonal ordered phase Ti_6C_5 with the packing defects characteristic of the 4H polytype was found in the Ti–C thin films.[130] The translation vectors of the unit cell are as follows: $\mathbf{a} = \{2\bar{1}\bar{1}\}_{B1}$, $\mathbf{b} = \{\bar{1}2\bar{1}\}_{B1}$ and $\mathbf{c} = \{111\}_{B1}$. The films were prepared by electron beam sputtering of sintered carbide $TiC_{0.9}$, by magnetron sputtering of titanium and carbon and by laser beam sputtering of titanium and graphite or carbide $TiC_{0.9}$. The ordered phase Ti_6C_5 corresponds to disordered carbide $TiC_{0.83}$ with a lattice constant, a_{B1}, of 0.4326 nm; however, the lattice parameters of the hexagonal ordered phase [130] correspond to disordered carbide TiC_y with the basis cubic lattice constant $a_{B1} = 0.4319$ nm characteristic of carbide $TiC_{0.68-0.70}$ (see Fig. 6). The underestimated a_{B1} value can be due to oxygen impurity.

Ordering of nonstoichiometric carbides MC_y can cause the formation of monoclinic and trigonal superstructures M_6C_5 with $C2/m$ (or $C2$) and $P3_1$ symmetry, respectively. The unit cell of monoclinic superstructure M_6C_5 (space group $C2/m$) is shown in Fig. 27 while its translation vectors and the atomic and vacancy coordinates are listed in Table 9. Translation of all superstructure

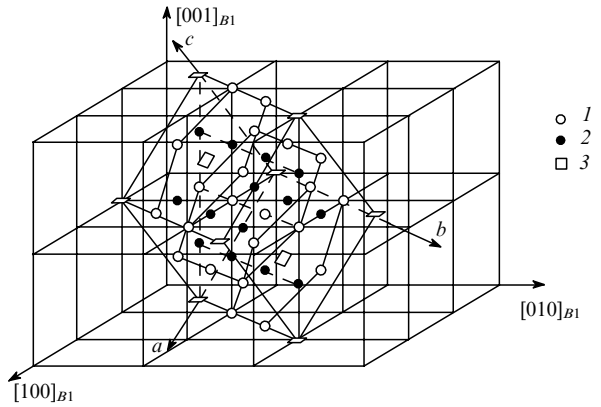


Figure 27. Monoclinic (space group $C2/m$) unit cell of the M_6C_5 superstructure in the crystal lattice with the $B1$-type structure. Interstitial atom (*1*), metal atom (*2*) and vacancy (*3*).[70, 126, 134]

Table 9. Characteristics of monoclinic [space group $C2/m$ (C_{2h}^3)] M_6C_5 superstructure: $\mathbf{a}_m = \frac{1}{2}\langle 1\bar{1}\bar{2}\rangle_{B1}$, $\mathbf{b}_m = \frac{3}{2}\langle 110\rangle_{B1}$, $\mathbf{c}_m = \frac{1}{2}\langle \bar{1}\bar{1}2\rangle_{B1}$.[70, 126, 134]

Atom	Position	Atomic coordinates in ideal ordered structure		
		x/a_m	y/b_m	z/c_m
C1 (vacancy)	2 (*a*)	0	0	0
C2	2 (*d*)	0	1/2	1/2
C3	4 (*g*)	0	1/3	0
C4	4 (*h*)	0	1/6	1/2
M1	4 (*i*)	1/4	0	3/4
M2	8 (*j*)	1/4	2/3	3/4

sites of the reciprocal lattice of the monoclinic ordered phase M_6C_5 (space group $C2/m$) showed that the first Brillouin zone of the disordered fcc lattice contains five inequivalent superstructure vectors belonging to three stars, $\{\mathbf{k}_9\}$, $\{\mathbf{k}_4\}$ and $\{\mathbf{k}_3\}$. These superstructure vectors are included in the MC_y (space group $Fm\bar{3}m$) $\rightleftharpoons$ M_6C_5 (space group $C2/m$) phase transition channel involving the formation of the monoclinic ordered phase M_6C_5.

The non-metal sublattice of the monoclinic superstructure M_6C_5 (space group $C2/m$) is divided into four inequivalent sublattices differing in site occupation probabilities by carbon atoms. Because of this, the non-metal sublattice is characterised by alternation of two types of non-metal atomic planes along the $[1\bar{1}1]_{B1}$ direction. In the first type of atomic planes one third of all sites belongs to the first sublattice while the other sites belong to the third sublattice, each site of the first sublattice being surrounded by six sites of the third sublattice. In the second type of planes one third of all sites belongs to the second sublattice while the other sites belong to the fourth sublattice; each site of the second sublattice is surrounded by six sites of the fourth sublattice.

The trigonal unit cell (space group $P3_1$) of superstructure M_6C_5 is shown in Fig. 28. Its translation vectors and the atomic and vacancy coordinates in ideal trigonal superstructure M_6C_5 are listed in Table 10. The disorder–order phase transition channel involving the formation of the trigonal superstructure M_6C_5 includes thirteen arms of three stars, $\{\mathbf{k}_9\}$, $\{\mathbf{k}_4\}$ and $\{\mathbf{k}_3\}$.

The unit cell of monoclinic superstructure M_6C_5 (space group $C2$) is presented in Fig. 29. The translation vectors of this unit cell and the atomic and vacancy coordinates in ideal monoclinic

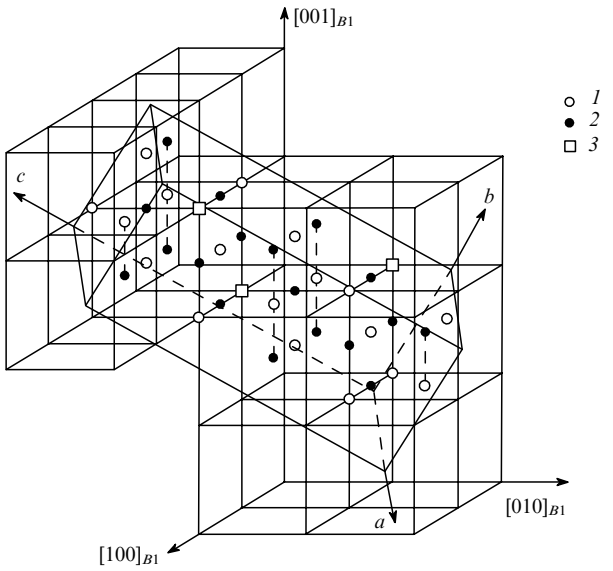


Figure 28. Trigonal (space group $P3_1$) unit cell of the M_6C_5 superstructure in the crystal lattice with the $B1$-type structure. Interstitial atom (*1*), metal atom (*2*) and vacancy (*3*).[70, 126, 134]

Table 10. Characteristics of trigonal [space group $P3_1$ (C_3^2)] M_6C_5 superstructure: $\mathbf{a}_{tr} = \frac{1}{2}\langle 21\bar{1}\rangle_{B1}$, $\mathbf{b}_{tr} = \frac{1}{2}\langle \bar{1}12\rangle_{B1}$, $\mathbf{c}_{tr} = 2\langle 1\bar{1}1\rangle_{B1}$.[70, 126, 134]

Atom	Position	Atomic coordinates in ideal ordered structure		
		x/a_{tr}	y/b_{tr}	z/c_{tr}
C1 (vacancy)	3 (*a*)	1/9	8/9	1/6
C2	3 (*a*)	4/9	5/9	1/6
C3	3 (*a*)	7/9	2/9	1/6
C4	3 (*a*)	1/9	5/9	1/3
C5	3 (*a*)	4/9	2/9	1/3
C6	3 (*a*)	7/9	8/9	1/3
M1	3 (*a*)	1/9	5/9	1/12
M2	3 (*a*)	4/9	2/9	1/12
M3	3 (*a*)	7/9	8/9	1/12
M4	3 (*a*)	1/9	2/9	1/4
M5	3 (*a*)	4/9	8/9	1/4
M6	3 (*a*)	7/9	5/9	1/4

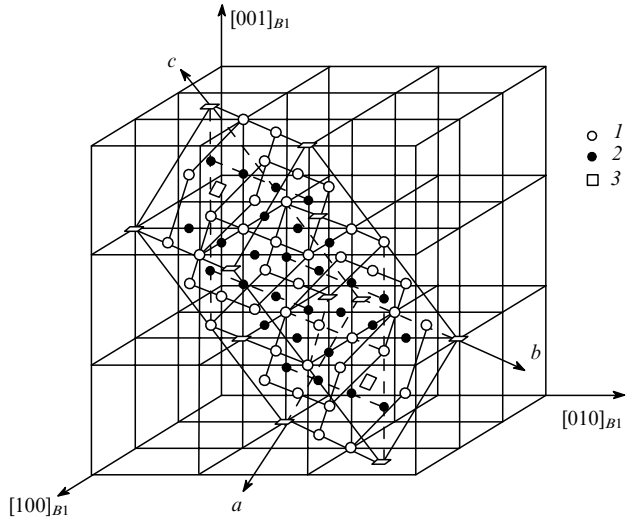


Figure 29. Monoclinic (space group *C*2) unit cell of the M_6C_5 superstructure in the crystal lattice with the *B*1-type structure. Interstitial atom (*1*), metal atom (*2*) and vacancy (*3*).[70, 126, 134]

superstructure M_6C_5 are given in Table 11. The transition channel involving the formation of this ordered phase M_6C_5 includes nine superstructure vectors of the reciprocal lattice belonging to four stars, $\{\mathbf{k}_9\}$, $\{\mathbf{k}_4\}$, $\{\mathbf{k}_3\}$ and $\{\mathbf{k}_0\}$. The non-metal sublattice of this superstructure is divided into five inequivalent sublattices and is characterised by alternation of two types of non-metal atomic planes along the $[1\bar{1}1]_{B1}$ direction. The first type of atomic plane contains an equal number of sites of the first, third and fifth sublattices, each site of a given sublattice being surrounded by the sites belonging to the other two sublattices. The second type of atomic plane is formed by the sites belonging to the second and fourth sublattices; here, each site of the fourth sublattice is surrounded by six sites of the second sublattice.

In Fig. 30 we present the X-ray diffraction patterns of the ideal, completely ordered monoclinic phases Ti_6C_5 (space groups $C2/m$ and $C2$) formed in titanium carbide $TiC_{0.83}$ ($a_{B1} = 0.4326$ nm). Positions and intensities of superstructure reflections in the X-ray diffraction pattern of the ideal, completely ordered trigonal phase Ti_6C_5 (space group $P3_1$, $a = b = 0.5299$, $c = 1.4987$ nm) match those of the monoclinic phase Ti_6C_5 (space group $C2/m$), since the transition channels involving the formation of both phases include the same superstructure vectors. For the real monoclinic and trigonal ordered phases Ti_6C_5, the intensities of superstructure reflections should be different due to

Table 11. Characteristics of monoclinic [space group $C2$ (C_3^3)] M_6C_5 superstructure: $\mathbf{a}_m = \frac{1}{2}\langle 1\bar{1}2\rangle_{B1}$, $\mathbf{b}_m = \frac{3}{2}\langle 110\rangle_{B1}$, $\mathbf{c}_m = \langle 1\bar{1}2\rangle_{B1}$.[70, 126, 134]

Atom	Position	Atomic coordinates in ideal ordered structure		
		x/a_m	y/b_m	z/c_m
C1 (vacancy)	2 (*a*)	0	0	0
C2 (vacancy)	2 (*b*)	0	1/3	1/2
C3	2 (*a*)	0	1/3	0
C4	2 (*a*)	0	2/3	0
C5	2 (*b*)	0	0	1/2
C6	2 (*b*)	0	2/3	1/2
C7	4 (*c*)	0	1/6	1/4
C8	4 (*c*)	0	1/2	1/4
C9	4 (*c*)	0	5/6	1/4
M1	4 (*c*)	1/4	1/6	1/8
M2	4 (*c*)	1/4	1/2	1/8
M3	4 (*c*)	1/4	5/6	1/8
M4	4 (*c*)	1/4	0	3/8
M5	4 (*c*)	1/4	1/3	3/8
M6	4 (*c*)	1/4	2/3	3/8

the difference between the directions and magnitudes of static atomic displacements. Analysis of the X-ray diffraction pattern taking into account these displacements allows unambiguous symmetry determination (monoclinic or trigonal) of the ordered phase Ti_6C_5.

The intensities of superstructure reflections of the Ti_6C_5 phases are very low: for instance, the intensity of the first superstructure reflection is 230–240 and 30–32 times lower than those of the $(111)_{B1}$ and $(222)_{B1}$ reflections, respectively. Comparison of the X-ray diffraction patterns of completely ordered phases Ti_2C

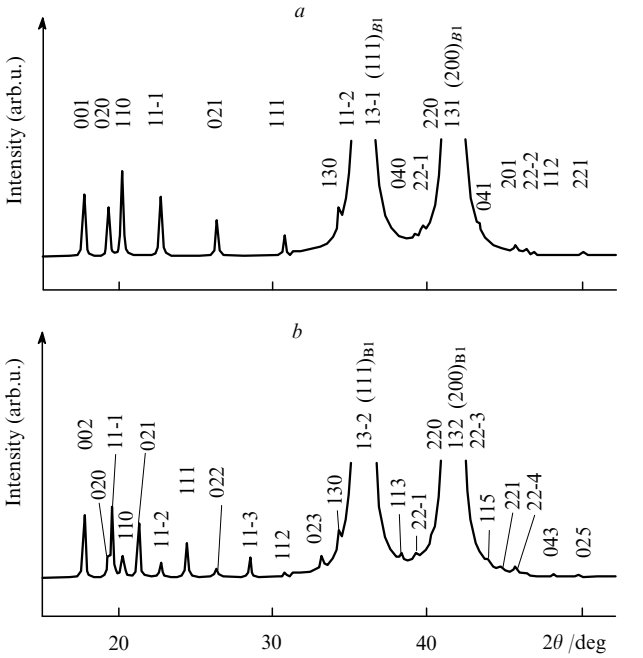


Figure 30. X-Ray diffraction patterns of completely ordered ($\eta = 1.00$), ideal monoclinic Ti_6C_5 phases (space group $C2/m$ and $C2$) formed in titanium carbide of composition $TiC_{0.83}$ ($a_{B1} = 0.4326$ nm). Calculated for $CuK_{\alpha 1,2}$ radiation.
Characteristics of the monoclinic Ti_6C_5 phase:
space group $C2/m$, $a = c = 0.5299$ nm, $b = 0.9177$ nm, $\beta = 109.47^\circ$ (*a*);
space group $C2$, $a = 0.5299$ nm, $b = 0.9177$ nm, $c = 1.0597$ nm, $\beta = 109.47^\circ$ (*b*).

and Ti_6C_5 shows that the intensity of the first superstructure reflection of the Ti_2C phase is nearly an order of magnitude higher than that of the Ti_6C_5 phase.

For all completely ordered phases M_6C_5 the relative stoichiometric concentration of interstitial atoms (y_{st}) equals 5/6. Consideration of the non-metal sublattices of these superstructures reveals that the $[1\bar{1}1]_{B1}$ direction is characterised by alternation of the $(1\bar{1}1)_{B1}$ atomic planes with completely occupied (by interstitial atoms) sites and the defect $(1\bar{1}1)_{B1}$ planes in which one third of sites is vacant (see Figs 27–29). Each vacancy is surrounded by six interstitial atoms that form a regular hexagon. Peculiarities of completely ordered carbide structures M_6C_5 have been studied in detail.[134]

Completely ordered monoclinic and trigonal carbide structures M_6C_5 with $C2/m$ (or $C2$) and $P3_1$ symmetry, respectively, are characterised by the identical environment of the metal atoms by the sites of the non-metal sublattice that form the first and second coordination spheres. Indeed, there are only two types of site for the metal atoms in these structures, *viz.*, M_1^1 (metal atom with one vacancy in the first and one vacancy in the second coordination sphere) and M_1^2 (metal atom with one vacancy in the first and two vacancies in the second coordination sphere). In ideal, completely ordered structures M_6C_5 (space groups $C2/m$, $P3_1$ and $C2$) two thirds of all metal atoms occupy the sites of the type M_1^1 while the other metal atoms occupy the sites of the type M_1^2.

V. Phase diagrams of the Ti – C system constructed with allowance for the ordering of TiC_y

The results of experimental,[14, 17, 70, 126, 127] theoretical[1–3, 12, 22, 135–137] and numerous structural studies of nonstoichiometric carbides MC_y with the $B1$-type basis structure including titanium carbide TiC_y revealed the possibility of formation of superstructures of the types M_2C, M_3C_2 and M_6C_5. Particular types of superstructures formed during the ordering of a given carbide MC_y and the corresponding concentration ranges are determined by the positions of the upper and lower boundaries of the homogeneity region of the disordered carbide and by the equilibrium conditions at these boundaries.

The most efficient method for calculating the low-temperature phase equilibria associated with the ordering of nonstoichiometric compounds is the above-mentioned OPF approach. Calculations of the phase diagram of an ordering system by this method require only knowledge of the $F_0(T)$, $F_1(T)$ and $F_2(T)$ parameters of the free energy $F(y,0,T)$ of disordered nonstoichiometric carbide MC_y. These parameters for TiC_y are listed in Section II.2.

According to the results of thermodynamic calculations[8, 60, 65] and crystal structure analysis,[4] the M_2X_3, M_4X_3, M_6X_5 and M_8X_7 superstructures can be formed by the first-order phase transition mechanism, whereas the M_2X superstructure can be formed by the second-order phase transition mechanism. Transition between two ordered phases occurs as a first-order phase transition.

1. Calculated phase diagrams of the Ti – C system

Let us consider the phase diagram of the Ti–C system obtained from the OPF calculations with allowance for the ordering of nonstoichiometric titanium carbide TiC_y.[1, 20]

There is only one compound capable of ordering in the Ti–C system, cubic carbide TiC_y. At the lower boundary of the homogeneity region, titanium carbide is in equilibrium with metallic α-Ti (at $T < 1150$ K) or β-Ti (at $T > 1150$ K). According to calculations,[18] at $1000 < T < 1900$ K the carbide that exists near the lower boundary of the homogeneity region of the disordered phase TiC_y has composition $TiC_{0.32}$–$TiC_{0.37}$. The exact position of the lower boundary of the homogeneity region has not experimentally been determined so far; different estimates gave $TiC_{0.48}$ (see Ref. 8) or $TiC_{0.47}$ (see Ref. 41) at 1900 K. According to calculations,[44] at 1900 K near the lower boundary of the homogeneity region the carbide has a $TiC_{0.52}$ composition. Calculations[8, 41, 44] revealed that as the temperature is lowered, the lower boundary of the homogeneity region of disordered TiC_y is shifted towards the region with higher y at a rate that is somewhat higher than that predicted by calculations.[18]

The low-temperature portion of the phase diagram of the Ti–C system, corresponding to the ordering of carbide TiC_y, was calculated by the OPF method.[18, 20]

The broad homogeneity region of TiC_y allows the formation of phases of the types Ti_2C, Ti_3C_2 and Ti_6C_5 (Fig. 31) during the ordering under thermodynamic equilibrium conditions. According to calculations, an ordered phase Ti_2C is formed by the second-order phase transition mechanism with the disorder–order transition temperature $T_{trans} = 920$–950 K. The homogeneity region of the Ti_2C phase is fairly broad ($TiC_{0.42}$–$TiC_{0.56}$ at 700 K and $TiC_{0.40}$–$TiC_{0.54}$ at 800 K) and is confined from the left and from the right by two-phase regions, (α-Ti + Ti_2C) and (Ti_2C + Ti_3C_2), respectively. The ordered Ti_3C_2 and Ti_6C_5 phases have homogeneity regions of comparable width ($TiC_{0.59}$–$TiC_{0.71}$ for Ti_3C_2 and $TiC_{0.74}$–$TiC_{0.87}$ for Ti_6C_5 at 700 K) and are formed by the first-order phase transition mechanism. All order–order phase transformations in titanium carbide also occur as first-order phase transitions. The calculated values of T_{trans}, ΔS_{trans} and the heat of phase transition, ΔH_{trans}, for all possible order–order and disorder–order first-order phase transformations of titanium carbide are listed in Table 12. By and large, the ordering in carbide TiC_y occurs at $T < 1000$ K.

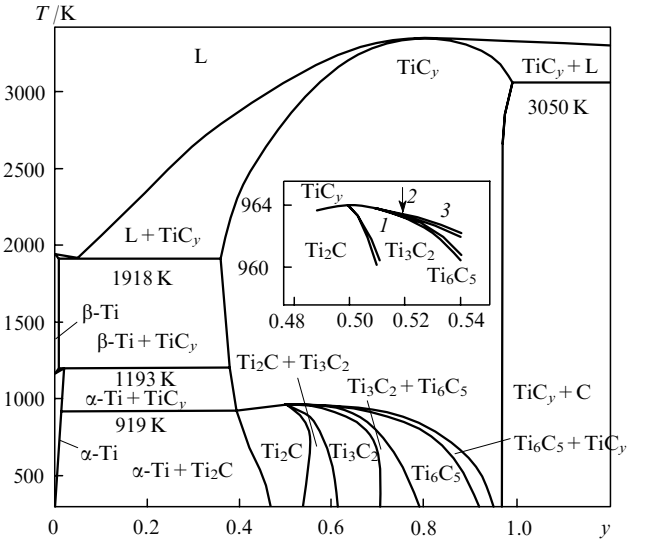


Figure 31. Equilibrium phase diagram of the Ti–C system constructed with allowance for atomic ordering of nonstoichiometric cubic titanium carbide TiC_y (see Ref. 1). A portion of the ordering region corresponding to peritectoid transformation $Ti_3C_2 + TiC_y \rightarrow Ti_6C_5$ ($T = 963$ K) is shown in the inset (magnified); the coordinates, y = C/Ti, of points *1*, *2* and *3* are 0.5236, 0.524 and 0.5255, respectively.

The calculated phase diagram of the Ti–C system (see Fig. 31) is in agreement with the results of experimental studies (see Section IV). Different authors reported the formation of an ordered phase Ti_2C with cubic or trigonal symmetry (space group $Fd\bar{3}m$ or $R\bar{3}m$, respectively) in carbide TiC_y in the region $0.5 \leqslant y \leqslant 0.65$ at $T < 1100$ K. The X-ray diffraction patterns of annealed titanium carbide of composition $TiC_{0.60}$–$TiC_{0.70}$ exhibited superstructure reflections characteristic of the ordered phase Ti_3C_2. Recently,[130] an ordered phase Ti_6C_5 with hexagonal symmetry was found in thin Ti–C films.

The existence of a trigonal ordered phase Ti_2C and an orthorhombic ordered phase Ti_3C_2 was also confirmed by the Monte Carlo calculations of the phase diagram of the Ti–C system for the composition range $TiC_{0.57}$–$TiC_{0.70}$ (Fig. 32).[10, 12] Landesman *et at.*[138] showed that short-range order and disorder–

Table 12. Thermodynamic characteristics of the disorder – order and order – order phase transformations in nonstoichiometric titanium carbide TiC_y (see Ref. 1).

y	$Ti_2C-Ti_3C_2$			$Ti_3C_2-Ti_6C_5$			$Ti_6C_5-TiC_y$		
	T_{trans} /K	ΔS_{trans} /J mol^{-1} K^{-1}	ΔH_{trans} /kJ mol^{-1}	T_{trans} /K	ΔS_{trans} /J mol^{-1} K^{-1}	ΔH_{trans} /kJ mol^{-1}	T_{trans} /K	ΔS_{trans} /J mol^{-1} K^{-1}	ΔH_{trans} /kJ mol^{-1}
0.52	948	0.09	0.08	–	–	–	–	–	–
0.53	926	0.15	0.14	961	0.003	0.003	962	0.02	0.02
0.54	893	0.25	0.22	959	0.013	0.013	961	0.03	0.03
0.55	853	0.28	0.24	956	0.03	0.03	960	0.04	0.04
0.56	795	0.32	0.25	951	0.05	0.05	959	0.06	0.05
0.58	460	0.29	0.13	940	0.12	0.12	955	0.10	0.09
0.60	–	–	–	924	0.19	0.18	949	0.15	0.14
0.62	–	–	–	902	0.29	0.26	942	0.22	0.21
0.63	–	–	–	891	0.35	0.31	938	0.26	0.24
0.64	–	–	–	877	0.41	0.36	934	0.30	0.28
0.65	–	–	–	860	0.48	0.42	929	0.35	0.32
0.66	–	–	–	841	0.56	0.47	924	0.40	0.37
0.68	–	–	–	794	0.74	0.59	912	0.50	0.46
0.70	–	–	–	733	0.91	0.66	898	0.62	0.56
0.72	–	–	–	639	0.99	0.63	882	0.75	0.67
0.73	–	–	–	566	1.00	0.57	874	0.82	0.72
0.74	–	–	–	472	0.90	0.42	864	0.90	0.78
0.75	–	–	–	320	0.69	0.22	854	0.97	0.83
0.76	–	–	–	–	–	–	843	1.05	0.88
0.78	–	–	–	–	–	–	818	1.20	0.98
0.80	–	–	–	–	–	–	789	1.34	1.06
0.82	–	–	–	–	–	–	755	1.46	1.10
0.83	–	–	–	–	–	–	728	1.49	1.08
0.84	–	–	–	–	–	–	713	1.49	1.07
0.85	–	–	–	–	–	–	689	1.48	1.02
0.86	–	–	–	–	–	–	662	1.43	0.95
0.88	–	–	–	–	–	–	601	1.27	0.76
0.90	–	–	–	–	–	–	528	1.05	0.55
0.92	–	–	–	–	–	–	444	0.82	0.36
0.94	–	–	–	–	–	–	348	0.58	0.20
0.95	–	–	–	–	–	–	294	0.46	0.14

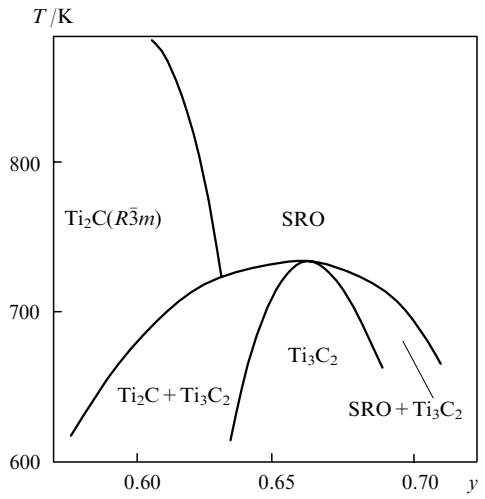


Figure 32. Portion of the phase diagram of the Ti – C system obtained from Monte Carlo calculations with allowance for the ordering of nonstoichiometric titanium carbide TiC_y in the composition range $TiC_{0.57}$ – $TiC_{0.70}$ (see Refs 10, 12).
SRO denotes a phase with the $B1$-type structure and short-range order.

order transitions in nonstoichiometric carbides and nitrides can be described by using the Ising Hamiltonian for the non-metal fcc sublattice. In this case the Hamiltonian is defined as the sum of the effective energies, V_n, of the pairwise interactions between the sites in the non-metal sublattice that are the nth meighbours. The energies V_n of the pairwise interactions in the non-metal sublattice of the carbides $TiC_{0.76}$ and $TiC_{0.65}$ were calculated [10, 12] not only for the nearest (V_1) and next-nearest (V_2) neighbours, but also for more distant sites in the third (V_3) and fourth (V_4) coordination spheres. The energies of the pairwise interactions were calculated from the experimental data on high-temperature diffuse neutron scattering [139] using three methods, namely, the mean field approximation, the inverse Monte Carlo method and the cluster variation method. The best agreement with the experiment was achieved when the phase diagram was calculated by the Monte Carlo method. The formation of an ordered orthorhombic phase Ti_3C_2, was reported to occur as a first-order phase transition.[12, 139] This conclusion is consistent with the results of OPF calculations of the ordering in TiC_y.[18, 20]

Some distinctions in the mutual positions of the ordered phases Ti_2C and Ti_3C_2 in the phase diagrams of the Ti – C system obtained from the OPF (see Fig. 31) and Monte Carlo calculations (see Fig. 32) are due to the fact that the OPF method treats the free energy of a compound as a function of its composition and long-range order parameters, whereas in the second method the energies of the interatomic interactions are determined by the short-range order parameters.

2. Experimental phase diagram of the Ti – C system constructed with allowance for low-temperature (at $T < 1000$ K) equilibria

The phase diagram of the Ti – C system at $T < 1000$ K was constructed based on the experimental results on the ordering of carbide TiC_y.[21] Using the data on the structure and electrical

resistance of annealed and quenched samples of TiC_y, it was shown that cubic ordered phase Ti_2C (space group $Fd\bar{3}m$) has a homogeneity region extending from $TiC_{0.49-0.51}$ to $TiC_{0.54-0.55}$, while the trigonal superstructure Ti_2C (space group $R\bar{3}m$) is formed in the composition range $TiC_{0.55}-TiC_{0.59}$. The $TiC_{0.59}-TiC_{0.63}$ range corresponds to a two-phase region [Ti_2C (space group $R\bar{3}m$) + Ti_3C_2 (space group $C222_1$)]. The existence region of the orthorhombic ordered phase Ti_3C_2 (space group $C222_1$) is fairly narrow and does not exceed $TiC_{0.63}-TiC_{0.67}$. The lowest annealing temperature was 770 K. Since no ordered phase Ti_6C_5 was detected after annealing the $TiC_{0.83}$ and $TiC_{0.85}$ samples at such a low temperature, the transition temperature of this phase was assumed to be lower than 770 K. The portion of the equilibrium phase diagram of the Ti–C system corresponding to the ordering of nonstoichiometric titanium carbide TiC_y is presented in Fig. 33. A consecutive transition was suggested [21] in the range $0.54 \leqslant y \leqslant 0.57$

disordered (space group $Fm\bar{3}m$) carbide TiC_y $\overset{990\pm20\ K}{\rightleftharpoons}$

$\rightleftharpoons$ cubic (space group $Fd\bar{3}m$) ordered phase Ti_2C $\overset{960\pm20\ K}{\rightleftharpoons}$

$\rightleftharpoons$ trigonal (space group $R\bar{3}m$) ordered phase Ti_2C.

The ordered orthorhombic phase Ti_3C_2 is formed following a peritectoid reaction

$$Ti_2C + TiC_y \longrightarrow Ti_3C_2$$

at 990 ± 10 K in the composition range $0.61 \leqslant y < 0.63$. The ordered phases Ti_2C with cubic and trigonal symmetry can be observed over a broad composition range of nonstoichiometric titanium carbide, from $TiC_{0.40}$ to $TiC_{0.63}$. However, only in the $TiC_{0.49-0.50}-TiC_{0.58-0.59}$ range is the homogeneity region of the ordered phase Ti_2C (see Fig. 33). The composition range in which the formation of an ordered phase Ti_6C_5 is possible is shown tentatively since this phase was not found experimentally. The hysteresis in the temperature dependences of the electrical resistance [21] suggested that the $TiC_y \rightleftarrows Ti_2C$ and $TiC_y \rightleftarrows Ti_3C_2$ transformations are first-order phase transitions with $T_{trans} = 980-1000$ K. This value is in good agreement with the value $T_{trans} \approx 1000$ K found for titanium carbide $TiC_{0.55}$ from electrical resistance measurements.[140]

Thus, experiments revealed that ordering of TiC_y in the ranges $0.52 \leqslant y \leqslant 0.55$, $0.56 \leqslant y \leqslant 0.58$ and $0.62 \leqslant y < 0.68$ at $T < 1000$ K leads respectively to the formation of the cubic (space group $Fd\bar{3}m$) and trigonal (space group $R\bar{3}m$) ordered phase Ti_2C and orthorhombic ordered phase Ti_3C_2 (space group $C222_1$). This is consistent with the phase diagram of the Ti–C system (see Fig. 31) obtained from OPF calculations [18] (note that for Ti_2C-type superstructures the OPF method leads to a common region of existence, from $TiC_{0.46}$ to $TiC_{0.58}$, without separation into the cubic and trigonal phases).

As mentioned above (see Section III), recent studies of the Ti–C system revealed the existence of molecular cluster-like compounds Ti_8C_{12} and $Ti_{13}C_{22}$ in addition to nonstoichiometric cubic titanium carbide TiC_y. The phase diagram of the Ti–C system constructed with allowance for the ordering of nonstoichiometric carbide TiC_y and for the existence of molecular cluster-like compounds Ti_8C_{12} and $Ti_{13}C_{22}$ (TiC_2) is shown in Fig. 34.

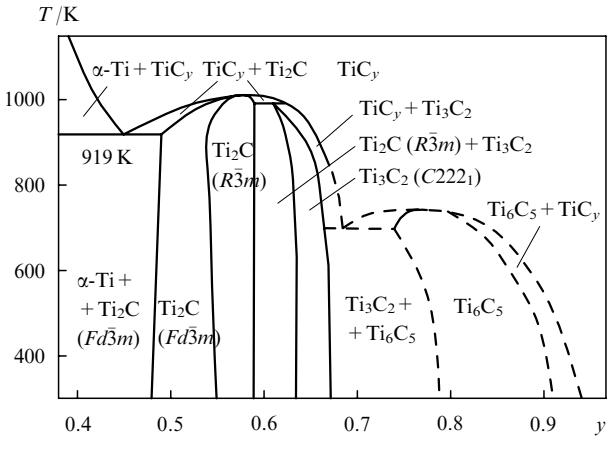


Figure 33. Low-temperature portion of the equilibrium phase diagram of the Ti–C system.[21]
Formation of the ordered orthorhombic Ti_3C_2 phase occurs at 990 ± 10 K as the peritectoid transformation $Ti_2C + TiC_y \rightarrow Ti_3C_2$; the region of phase equilibria involving ordered Ti_6C_5 phase is tentatively shown by the dashed line.

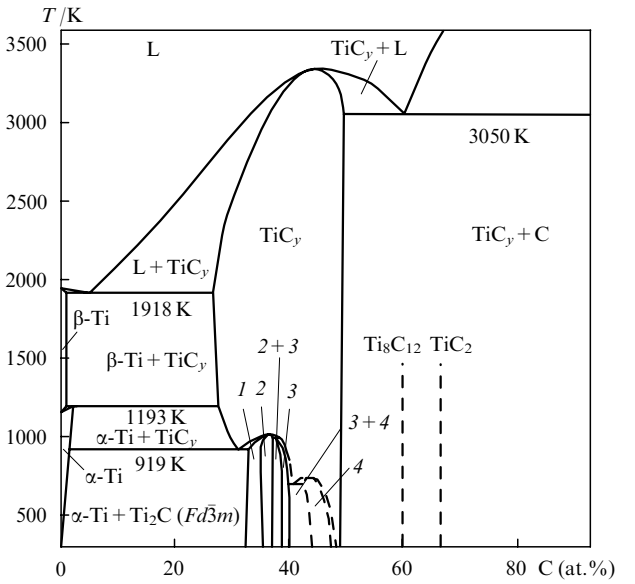


Figure 34. Phase diagram of the Ti–C system constructed with allowance for the existence of molecular cluster-like compounds Ti_8C_{12} and $Ti_{13}C_{22}$ (TiC_2) and for the atomic ordering of nonstoichiometric cubic titanium carbide TiC_y.
Ti_2C (space group $Fd\bar{3}m$) (*1*), Ti_2C (space group $R\bar{3}m$) (*2*), Ti_3C_2 (space group $C222_1$) (*3*) and Ti_6C_5 (Ti_2C, Ti_3C_2 and Ti_6C_5 are the ordered phases of titanium carbide TiC_y) (*4*).

VI. Conclusion

For more than a century it was thought that there is only one compound in the Ti–C system, namely, cubic titanium carbide TiC_y with a broad homogeneity region. However, the studies of this system carried out in 1990s revealed the formation of (i) ordered phases of nonstoichiometric titanium carbide with different composition and symmetry and (ii) molecular cluster-like compounds.

Among the new phases of titanium carbide, the ordered phase Ti_2C, which can have a cubic or trigonal symmetry, has been studied in most detail. This phase is readily formed as a result of annealing the TiC_y samples at 1300–1500 K followed by gradual lowering of the temperature down to 600–700 K over a period of several hours. It can also be found even in the TiC_y samples ($y = 0.5-0.58$) synthesised by solid-phase vacuum sintering of titanium and carbon at 2000–2200 K and cooled down to 300 K during further self-cooling of the furnace. Using a special regime of long-term annealing, one can obtain the Ti_2C phase with the maximum extent of long-range order.

Ordered phases of the Ti_3C_2 and Ti_6C_5 types are much more hard to obtain. Similar to the Ti_2C phase, they can be of different symmetry while their chemical composition remains unchanged.

Bulk samples of these phases can be obtained only after long-term (several hundreds of hours) annealing at $T < 1000$ K. The results of experimental and theoretical studies suggest that these phases are in thermodynamic equilibrium at temperatures below 900–1000 K. A hexagonal Ti_6C_5 phase was found in thin films synthesised by electron beam and laser sputtering of titanium carbide.

Molecular cluster-like compounds Ti_8C_{12} (Ti_2C_3) and $Ti_{13}C_{22}$ ($\sim TiC_2$) were obtained by laser-assisted plasmachemical synthesis. The most convenient procedure for preparation of these compounds in the crystalline form is to stabilise them in thin films deposited on a substrate (molecular clusters with a characteristic atomic ratio, C : Ti = 1.5 or 2).[141] This allows one to obtain thin films of a compound Ti_2C_3 or TiC_2 with the crystal structure similar to that of the substrate. Indeed, the synthesis of titanium oxide, fullerene and amorphous carbon nanocrystals with a different structure on the solid surfaces of different chemical nature (graphite, polymers, oxides) was reported.[142] Chemical modification of the substrate surface or heat treatment of the film cast provide additional possibilities of forming a particular type of the crystal structure of the film.

The main methods of experimental detection of new compounds and phases include X-ray, electron or neutron diffraction. We believe that the model X-ray diffraction patterns of most of the phases of the Ti–C system, first reported in this review will essentially facilitate identification of new phases and interpretation of the results obtained.

Thus, analysis of studies on the Ti–C system carried out in 1985–2000 showed that not only titanium carbide TiC_y, but also other chemical compounds and phases are formed in this system. They were discovered using novel, advanced methods of synthesis, thorough studies of phase equilibria at temperatures below 1300 K and highly sensitive mass spectrometric and diffraction methods of analysis of products of the chemical interaction. One can expect (and some experimental proofs have already been reported) that binary systems comprising carbon and other transition metals can appear to be no less interesting than the Ti–C system.

This work has been written with the financial support of the Russian Foundation for Basic Research (Project No. 01-03-96510).

References

1. A I Gusev *Usp. Fiz. Nauk* **170** 3 (2000) [a]
2. A I Gusev, A A Rempel, A J Magerl *Disorder and Order in Strongly Nonstoichiometric Compounds: Transition Metal Carbides, Nitrides and Oxides* (Berlin; Heidelberg; New York; London: Springer, 2001)
3. A I Gusev, A A Rempel *Nestekhiometriya, Besporyadok i Poryadok v Tverdom Tele* (Nonstoichiometry, Disorder and Order in Solid) (Ekaterinburg: Urals Branch of the Russian Academy of Sciences, 2001)
4. P W Shimer *Proc. R. Soc.* **42** 89 (1887)
5. P W Shimer *Chem. News* **55** 156 (1887)
6. H Moissan *Compt. Rend.* **120** 290 (1895)
7. E Rudy, D P Harmon, C E Brukl, in *Ternary Phase Equilibria in Transition Metal-Boron-Carbon-Silicon Systems. Related Binary Systems (Tech. Report AFML-TR-65-2)* Vol. 2, Pt. I (Ohio, USA: Metals and Ceramics Division, Air Force Materials Laboratory Wright-Patterson Air Force Base, 1965) p. 1
8. E K Storms *The Refractory Carbides* (New York; London: Academic Press, 1967)
9. H Goretzki *Phys. Status Solidi* **20** K141 (1967)
10. T Priem *Etude de L'ordre a Courte Distance Dans les Carbures et Nitrures Non-Stoechiometriques de Metaux de Transition par Diffusion Diffuse de Neutrons (Rapport CEA-R-5499)* (Gif-sur-Yvette: Commissariat a l'Energie Atomique Centre d'Etudes Nucleaires de Saclay, 1989)
11. A I Gusev *Dokl. Akad. Nauk SSSR* **313** 887 (1990) [b]
12. C H de Novion, B Beuneu, T Priem, N Lorenzelli, A Finel, in *The Physics and Chemistry of Carbides, Nitrides and Borides* (Ed. R Freer) (Netherlands: Kluwer Academic, 1990) p. 329
13. A I Gusev *Fiz. Tv. Tela* **32** 2752 (1990) [c]
14. A I Gusev *Fizicheskaya Khimiya Nestekhiometricheskikh Tugoplavkikh Soedinenii* (Physical Chemistry of Nonstoichiometric Refractory Compounds) (Moscow: Nauka, 1991)
15. A I Gusev, A A Rempel' *Zh. Fiz. Khim.* **65** 625 (1991) [d]
16. A I Gusev *Dokl. Akad. Nauk* **322** 918 (1992) [b]
17. A A Rempel' *Effekty Uporyadocheniya v Nestekhiometricheskikh Soedineniyakh Vnedreniya* (The Ordering Effects in Nonstoichiometric Intercalation Compounds) (Ekaterinburg: Nauka, 1992)
18. A I Gusev, A A Rempel *Dokl. Akad. Nauk* **332** 717 (1993) [b]
19. A I Gusev, A A Rempel *J. Phys. Chem. Solids* **55** 299 (1994)
20. A I Gusev, A A Rempel *Phys. Status Solidi A* **163** 273 (1997)
21. V N Lipatnikov, A Kottar, L V Zueva, A I Gusev *Fiz. Tv. Tela* **40** 1332 (1998) [c]
22. A I Gusev, A A Rempel, in *Materials Science of Carbides, Nitrides and Borides* (Eds Y G Gogotsi, R A Andrievski) (Dordrecht: Kluwer Academic, 1999) p. 47
23. V N Lipatnikov, A I Gusev, P Ettmayer, W Lengauer *J. Phys., Condens. Matter* **11** 163 (1999)
24. V N Lipatnikov, A I Gusev, P Ettmaier, V Lengauer *Fiz. Tv. Tela* **41** 529 (1999) [c]
25. A I Gusev *Dokl. Akad. Nauk* **365** 644 (1999) [b]
26. A I Gusev *Zh. Fiz. Khim.* **74** 600 (2000) [d]
27. V N Lipatnikov, A I Gusev *Uporyadochenie v Karbidakh Titana i Vanadiya* (Ordering in Titanium and Vanadium Carbides) (Ekaterinburg: Urals Branch of the Russian Academy of Sciences, 2000)
28. B C Guo, K P Kerns, A W Castleman *Science* **255** 1411 (1992)
29. Z Lin, M B Hall *J. Am. Chem. Soc.* **115** 11165 (1993)
30. B C Guo, S Wei, J Purnell, S Buzza, A W Castleman Jr *Science* **256** 515 (1992)
31. S Wei, B C Guo, J Purnell, S Buzza, A W Castleman *J. Phys. Chem.* **96** 4166 (1992)
32. J S Pilgrim, M A Duncan *J. Am. Chem. Soc.* **115** 4395 (1993)
33. B C Guo, A W Castleman *Adv. Met. Semicond. Clusters* **2** 137 (1994)
34. A W Castleman *Proc. Electrochem. Soc.* **92–94** 346 (1994)
35. M Methfessel, M van Schilfgaarde, S Scheffler *Phys. Rev. Lett.* **70** 29 (1993)
36. B V Reddy, S N Khanna, P Jena *Science* **258** 1640 (1992)
37. M V Ryzhkov, A L Ivanovskii *Zh. Strukt. Khim.* **40** 630 (1999) [e]
38. S N Khanna, B V Reddy *Comput. Mater. Sci.* **2** 638 (1994)
39. E Rudy, in *Compendium of Phase Diagram Data. Metals and Ceramics Division (Final Tech. Report AFML TR-65-2)* (Ohio, USA: Air Force Materials Laboratory, Wright-Patterson Air Force Base, 1969) Pt. V
40. R L Bickerdike, G L Hughes *J. Less-Common Met.* **1** 42 (1959)
41. J L Murray, in *Phase Diagrams of Binary Titanium Alloys* (Ed. J L Murray) (Metals Park, OH: ASM Int. Publ., 1987) p. 47
42. J L Murray, in *Binary Alloy Phase Diagrams* Vol. 1 (Ed. T B Massalski) (Metals Park, OH: ASM Int. Publ., 1987) p. 593
43. T B Massalski, P R Subramanian, H Okamoto, L Kasprzak (Eds) *Binary Alloy Phase Diagrams* Vol. 1 (Metals Park, OH: ASM Int. Publ., 1990)
44. S Jonsson, PhD Thesis, Royal Institute of Technology, Stockholm, 1993
45. H Bittner, H Goretzki *Monatsh. Chem.* **93** 1000 (1962)
46. M P Arbuzov, B V Khaenko, E T Kachkovskaya, S Ya Golub *Ukr. Fiz. Zh.* **19** 497 (1984)
47. V T Em, I A Karimov, V F Petrunin, I Khidirov, I S Latergaus, A G Merzhanov, I P Borovinskaya, V K Prokudina *Kristallografiya* **20** 320 (1975) [f]
48. I Karimov, V T Em, I Khidirov, I S Latergaus *Izv. Akad. Nauk Uzb. SSR, Ser. Fiz.-Mat. Nauk* (4) 81 (1979)
49. V Moisy-Maurice, N Lorenzelli, C H de Novion, P Convert *Acta Metall.* **30** 1769 (1982)
50. A Sh Remeev, I Karimov *Izv. Akad. Nauk Uzb. SSR, Ser. Fiz.-Mat. Nauk* (2) 87 (1986)
51. V A Vlasov, I A Karimov, L V Kustova *Izv. Akad. Nauk SSSR, Neorg. Mater.* **22** 231 (1986) [g]
52. A N Emel'yanov *Teplofiz. Vys. Temp.* **28** 269 (1990) [h]

53. A V Karpov, V P Kobyakov, E A Chernomorskaya *Neorg. Mater.* **31** 655 (1995) [g]
54. A V Karpov, V P Kobyakov *Fiz. Tv. Tela* **38** 1638 (1996) [c]
55. V N Lipatnikov, A I Gusev *Phys. Status Solidi B* **212** R11 (1999)
56. V N Lipatnikov, A I Gusev *Pis'ma Zh. Eksp. Teor. Fiz.* **69** 631 (1999) [i]
57. L V Zueva, A I Gusev *Fiz. Tv. Tela* **41** 1134 (1999) [c]
58. G L Humphrey *J. Am. Chem. Soc.* **73** 2261 (1951)
59. M P Morozova, M K Khripun, S M Ariya *Zh. Obshch. Khim.* **32** 2072 (1962) [j]
60. A N Zyryanova, L V Zueva, A I Gusev, in *Khimiya Tverdogo Tela. Struktura, Svoistva i Primenenie Novykh Neorganicheskikh Materialov* (The Solid State Chemistry. Structure, Properties and Application of New Inorganic Materials) (Ekaterinburg: Institute of Solid State Chemistry, Urals Branch of the Russian Academy of Sciences, 1998) p. 36
61. L V Zueva, A I Gusev *Zh. Fiz. Khim.* **73** 792 (1999) [d]
62. B Naylor *Am. Chem. Soc.* **68** 370 (1946)
63. L S Levinson *J. Chem. Phys.* **42** 2891 (1965)
64. V V Fesenko, A G Turchanin, E A Guseva *Zh. Fiz. Khim.* **42** 1026 (1968) [d]
65. V V Fesenko, A G Turchanin, in *Tugoplavkie Karbidy* (The Refractory Carbides) (Kiev: Naukova Dumka, 1970) p. 200
66. V E Ganenko, G A Berezovskii, V S Neshpor, G M Klimashin, in *Raboty po Fizike Tverdogo Tela* (Studies on Physics of Solid State) (Novosibirsk: Nauka, 1968) Vol. 3, p. 127
67. N Lorenzelli, R Caudron, J P Landesman, C H de Novion *Solid State Commun.* **59** 765 (1986)
68. V P Glushko (Ed.) *Termodinamicheskie Svoistva Individual'nykh Veshchestv. Spravochnik* (Thermodynamic Properties of Individual Compounds. Handbook) (Moscow: Nauka, 1979) Vol. 2, Pts 1, 2
69. R B Kotel'nikov, S N Bashlykov, Z G Galiakbarov, A I Kashtanov *Osobo Tugoplavkie Elementy i Soedineniya* (Especially Refractory Elements and Compounds) (Moscow: Metallurgiya, 1969)
70. A I Gusev, A A Rempel *Strukturnye Fazovye Perekhody v Nestekhiometricheskikh Soedineniyakh* (Structural Phase Transitions in Nonstoichiometric Compounds) (Moscow: Nauka, 1988)
71. J P Hirth, G M Pound *Condensation and Evaporation-Nucleation and Growth Kinetics* (Oxford: Pergamon Press, 1963)
72. A I Gusev *Dokl. Akad. Nauk SSSR* **311** 631 (1990) [b]
73. A I Gusev *Teplofiz. Vys. Temp.* **29** 695 (1991) [h]
74. W A Chupka, J Berkowitz, C F Giese, M G Inghram *J. Phys. Chem.* **62** 611 (1958)
75. T S Starostina, L N Sidorov, P A Akishin, N M Karasev *Izv. Akad. Nauk SSSR, Neorg. Mater.* **3** 727 (1967) [g]
76. S Fujishiro, N A Gokcen *J. Phys. Chem.* **65** 161 (1961)
77. C A Stearns, F J Kohl *High Temp. Sci.* **2** 274 (1970)
78. I S Kulikov *Termodinamika Karbidov i Nitridov* (Thermodynamics of Carbides and Nitrides) (Chelyabinsk: Metallurgiya, 1988)
79. V V Fesenko, A S Bolgar *Teplofiz. Vys. Temp.* **7** 244 (1969) [h]
80. A I Gusev, A A Rempel *Izv. Akad. Nauk SSSR, Neorg. Mater.* **27** 963 (1991) [g]
81. T Ya Kosolapova (Ed.) *Svoistva, Poluchenie i Primenenie Tugoplavkikh Soedinenii. Spravochnik* (Properties, Preparation and Applications of Refractory Compounds. Handbook) (Moscow: Metallurgiya, 1986)
82. H Gleiter *Nanostruct. Mater.* **1** 1 (1992)
83. R Birringer, H Gleiter, in *Encyclopedia of Material Science and Engineering (Suppl.)* Vol. 1 (Ed. R W Cahn) (Oxford: Pergamon Press, 1988) p. 339
84. R W Siegel *Ann. Rev. Mater. Sci.* **21** 559 (1991)
85. A I Gusev *Usp. Fiz. Nauk* **168** 55 (1998) [a]
86. Yu I Petrov *Fizika Malykh Chastits* (The Physics of Small Particles) (Moscow: Nauka, 1982)
87. H Gleiter, in *Deformation of Polycrystals: Mechanisms and Microstructures* (Roskilde: Risø National Laboratory, 1981) p. 15
88. H Gleiter, P Marquardt *Z. Met.kd.* **75** 263 (1984)
89. R Birringer, U Herr, H Gleiter *Trans. Jpn. Inst. Met. (Suppl.)* **27** 43 (1986)
90. H Gleiter *Prog. Mater. Sci.* **33** 233 (1989)
91. A I Gusev *Nanokristallicheskie Materialy: Metody Polucheniya i Svoistva* (Nanocrystalline Materials: Preparation Methods and Properties) (Ekaterinburg: Urals Branch of the Russian Academy of Sciences, 1998)
92. A I Gusev, A A Rempel *Nanokristallicheskie Materialy* (Nanocrystalline Materials) (Moscow: Fizmatlit-Nauka, 2000)
93. E Neuenschwander *J. Less-Common Met.* **11** 365 (1966)
94. T Ya Kosolapova, G N Makarenko, D P Zyat'kevich *Zh. Vsesoyuz. Khim. O-va im. D I Mendeleeva* **24** 228 (1979) [k]
95. J I Steinfeld (Ed.) *Laser-Induced Chemical Processes* (New York: Plenum, 1981)
96. R A Bauer, J G M Becht, F E Kruis, B Scarlett, J Schoonman *J. Am. Ceram. Soc.* **74** 2759 (1991)
97. M Suzuki, Y Maniette, Y Nakata, T Okutani *J. Am. Ceram. Soc.* **76** 1195 (1993)
98. N V Karlov, M A Kirichenko, B S Luk'yanchuk *Usp. Khim.* **62** 223 (1993) [*Russ. Chem. Rev.* **62** 203 (1993)]
99. A Teresiak, H Kubsch *Nanostruct. Mater.* **6** 671 (1995)
100. M S El-Eskandarany, M Omori, T Kamiyama, T J Konno, K Sumiyama, T Hirai, K Suzuki *Sci. Rep. Res. Inst. Tohoku Univ. A, Phys. Chem. Metall.* **43** 181 (1997)
101. R Z Valiev, A V Korznikov, R R Mulyukov *Mater. Sci. Eng. A* **168** 141 (1993)
102. A A Rempel, A I Gusev, R R Mulyukov, in *Ul'tradispersnye Poroshki, Materialy i Nanostruktury. Materialy Mezhregional'noi Konferentsii* (Ultradispersed Powders Materials and Nanostructures. Materials of International Conference) (Ed. V E Red'kin) (Krasnoyarsk: Krasnoyarsk State Technological University, 1996) p. 131
103. E A Rohlfing, D M Cox, A Kaldor *J. Chem. Phys.* **81** 3322 (1984)
104. H W Kroto, J R Heath, S C O'Brien, R F Curl, R E Smalley *Nature (London)* **318** 162 (1985)
105. R F Curl, R E Smalley *Science* **242** 1017 (1988)
106. H W Kroto, A W Allaf, S P Balm *Chem. Rev.* **91** 1213 (1991)
107. A V Eletskii, B M Smirnov *Usp. Fiz. Nauk* **165** 977 (1995) [a]
108. G S Hammond, V J Kuck (Eds) *Fullerenes. Synthesis, Properties, and Chemistry of Large Carbon Clusters. ACS Symposium Series* Vol. 481 (Washington, DC: American Chemical Society, 1992)
109. J H Weaver, J L Martins, T Komeda, Y Chen, T R Ono, G H Kroll, N Troullier, R E Haufler, R E Smalley *Phys. Rev. Lett.* **66** 1741 (1991)
110. S Saito, A Oshiyama *Phys. Rev. Lett.* **66** 2637 (1991)
111. B C Guo, K P Kerns, A W Castleman *J. Am. Chem. Soc.* **115** 7415 (1993)
112. A A Sofronov, Candidate Thesis in Chemical Sciences, Institute of Solid State Chemistry, Urals Branch of the Russian Academy of Sciences, Ekaterinburg, 2000
113. A L Ivanovskii, A A Sofronov, Yu N Makurin *Teor. Eksp. Khim.* **35** 289 (1999)
114. D W Jones, I J McColm, R Steadman, J Yerkess *J. Solid State Chem.* **68** 219 (1987)
115. S Raman, G N Ramanchandran *Curr. Sci., A* **31** 321 (1962)
116. V I Perekrestov, A V Pavlov *Pis'ma Zh. Eksp. Teor. Fiz.* **73** 17 (2001) [i]
117. M S Dresselhaus, G Dresselhaus, P C Eklund *Science of Fullerenes and Carbon Nanotubes* (San-Diego: Academic Press, 1996)
118. A L Buchachenko *Usp. Khim.* **68** 99 (1999) [*Russ. Chem. Rev.* **68** 85 (1999)]
119. T Guo, M D Diener, Y Chai, M J Alford, R E Hauter, S M McClure, T Ohto, J H Weaver, G E Scuseria, R E Smalley *Science* **257** 1661 (1992)
120. Yu N Makurin, A A Sofronov, A I Gusev, A L Ivanovskii *Chem. Phys.* **270** 293 (2001)
121. T Guo, R E Smalley, G E Scuseria *J. Chem. Phys.* **99** 352 (1993)
122. N A Dubrovinskaia, L S Dubrovinsky, S K Saxena, R Ahuja, B Johansson *J. Alloys Comp.* **289** 24 (1999)
123. B V Khaenko *Izv. Akad. Nauk SSSR, Neorg. Mmater.* **15** 1952 (1979) [g]
124. C H de Novion, J P Landesman *Pure Appl. Chem.* **57** 1391 (1985)
125. A I Gusev *Phys. Status Solidi B* **163** 17 (1991)
126. A I Gusev, A A Rempel *Phys. Status Solidi A* **135** 15 (1993)
127. A A Rempel *Usp. Fiz. Nauk* **166** 33 (1996) [a]
128. B V Khaenko, S Ya Golub, M P Arbuzov *Kristallografiya* **25** 112 (1980) [f]
129. V Moisy-Maurice, in *Structure Atomique des Carbures Non-stoechiometriques de Metaux de Transition (Rapport CEA-R-5127)* (Gif-sur-Yvette: Commissariat a l'Energie Atomique, 1981)

130. N V Dzhalabadze, B G Eristavi, N I Maisuradze, E R Kuteliya *Fiz. Met. Metalloved.* **86** 85 (1998) [m]
131. M Yu Tashmetov, V T Em, M U Kalanov, V M Shkiro *Metallofizika* **13** 100 (1991)
132. V N Lipatnikov, A A Rempel, A I Gusev *Int. J. Refract. Met. Hard Mater.* **15** 61 (1997)
133. V Moisy-Maurice, C H de Novion, A N Christensen, W Just *Solid State Commun.* **39** 661 (1981)
134. A I Gusev, A A Rempel *J. Phys. C, Solid State Phys.* **20** 5011 (1987)
135. A I Gusev, A A Rempel *Phys. Status Solidi B* **131** 43 (1985)
136. A I Gusev, A A Rempel *Phys. Status Solidi B* **140** 335 (1987)
137. A I Gusev *Philos. Mag. B* **60** 307 (1989)
138. J P Landesman, G Treglia, P Turchi, F Ducastelle *J. Phys. (France)* **46** 1001 (1985)
139. T Priem, B Beuneu, C H de Novion, J Chevrier, F Livet, A Finel, S Lefevbre *Physica B* **156** – **157** 47 (1989)
140. V N Lipatnikov, A I Gusev *Pis'ma Zh. Eksp. Teor. Fiz.* **70** 284 (1999) [i]
141. R B King *Izv. Akad. Nauk, Ser. Khim.* **5** 862 (1998) [n]
142. E P Smirnov, A M Abyzov, V Vege, in *Khimiya Vysokoorganizovannykh Veshchestv i Nauchnye Osnovy Nanotekhnologii (3-ya Mezhdunarodnaya Konferentsiya)* [The Chemistry of Highly Organised Substances and Scientific Foundations of Nanotechnology (The 3th International Conference)] (St Petersburg: St Petersburg State University, 2001) p. 58

[a] — *Physics-Uspekhi (Engl. Transl.)*
[b] — *Dokl. Chem. (Engl. Transl.)*
[c] — *Phys. Solid State (Engl. Transl.)*
[d] — *Russ. J. Phys. Chem. (Engl. Transl.)*
[e] — *J. Struct. Chem. (Engl. Transl.)*
[f] — *Crystallogr. Rep. (Engl. Transl.)*
[g] — *Inorg. Mater. (Engl. Transl.)*
[h] — *High Temp. (Engl. Transl.)*
[i] — *J. Exp. Theor. Phys. Lett. (Engl. Transl.)*
[j] — *Russ. J. Gen. Chem. (Engl. Transl.)*
[k] — *Mendeleev Chem. J. (Engl. Transl.)*
[m] — *Phys. Met. Metall. (Engl. Transl.)*
[n] — *Russ. Chem. Bull., Int. Ed. (Engl. Transl.)*